REPORT DOCUMENTATION PAGE

Form Approved
OMB No. 0704-0188

1. REPORT DATE (DD-MM-YYYY)	2. REPORT DATE	3. DATES COVERED (From - To)
28/05/2002	Final Technical	30/07/1997-31/07/2001

4. TITLE AND SUBTITLE
Investigation of the Growth of Lead Magnesium Niobate- and Lead Zinc Niobate-Lead Titanate Solid Solutiob Single Crystals by the Bridgman Technique

5a. CONTRACT NUMBER

5b. GRANT NUMBER
N00014-97-1-1000

5c. PROGRAM ELEMENT NUMBER

6. AUTHOR(S)
Feigelson, Robert S.

5d. PROJECT NUMBER

5e. TASK NUMBER

5f. WORK UNIT NUMBER

7. PERFORMING ORGANIZATION NAME(S) AND ADDRESS(ES)
Laboratory for Advanced Materials, Stanford University
476 Lomita Mall
Stanford, CA 94305-4045

8. PERFORMING ORGANIZATION REPORT NUMBER

9. SPONSORING/MONITORING AGENCY NAME(S) AND ADDRESS(ES)
Office of Naval Research Regional Office Seattle
]]07 NE 45th Street Suite 350
Seattle, WA 98]05-463]

10. SPONSOR/MONITOR'S ACRONYM(S)

11. SPONSORING/MONITORING AGENCY REPORT NUMBER

12. DISTRIBUTION AVAILABILITY STATEMENT
No Limitations

DISTRIBUTION STATEMENT A
Approved for Public Release
Distribution Unlimited

13. SUPPLEMENTARY NOTES

14. ABSTRACT
During this program the following milestones were achieved: 1) Developed a method for synthesizing near pyrochlore-free PMNT starting material for crystal growth using the Columbite process and Pb_3O_4. Pyrochlore-free starting material prevents the crystals from sticking to the walls of the Pt crucibles and thereby prevents some forms of cracking. An another important development was the use of commercial magnesium niobate that reduced the number of processing steps and time by 50%. 2) Measured the liquidus curve in the PMN-PT phase diagram system for the first time. 3) Grew the first large PMN and PMN 10PT single crystals from nonfluxed melts by the Bridgman method during the first year and had their properties measured. These crystals grew along the 111 direction, their fast growth axis and their properties were consistent with literature values, 4) Grew large, transparent one inch diameter boules of PMN-35PT and PMN-32PT crystals using seed crystals for evaluation of compositional and structural uniformity, crystalline defects, etc. Uniform axial and radial composition was found in one cm diameter boules but axial Ti concentration variations were over 10 % in one inch diameter crystals. Samples have been submitted for property measurements and evaluation to NUWC, Tetrad, Washington State University, Penn State University, Hewlett Packard, Wilcoxon, etc. It was found that the properties of the tetragonal PMNT phase (greater than 35% Ti) were not as good as those for rhombohedral crystals.

15. SUBJECT TERMS
Lead Magnesium Niobate-Lead Titanate, Solid Solutions, Single Crystals, Bridgman Technique

16. SECURITY CLASSIFICATION OF:			17. LIMITATION OF ABSTRACT	18. NUMBER OF PAGES	19a. NAME OF RESPONSIBLE PERSON
a. REPORT	b. ABSTRACT	c. THIS PAGE			Robert S. Feigelson
U	U	U	UU	42	19b. TELEPONE NUMBER (Include area code) 650 723-4007

Geballe Laboratory for Advanced Materials
McCullough Building
Stanford University,
Stanford CA 94305-4045

Final Technical Report

Report for the Period

7/30/97-7/31/01

on

INVESTIGATION OF THE GROWTH OF LEAD MAGNESIUM NIOBATE – AND LEAD ZINC NIOBATE - LEAD TITANATE SOLID SOLUTION SINGLE CRYSTALS BY THE BRIDGMAN TECHNIQUE

ONR Grant # N00014-97-1-1000

Submitted to
Office of Naval Research
Program Officers:
Dr. Wallace Smith and Dr. Carl Wu
Ballston Centre Tower One
Office of Naval Research
800 N. Quincy Street
Arlington, VA 22217-5660

PI: Robert S. Feigelson

Submitted by
The Board of Trustees of
The Leland Stanford Jr. University
Stanford, California 94305

May 30, 2002

TABLE OF CONTENTS

ABSTRACT

During this program the following milestones were achieved: 1) Developed a method for synthesizing near pyrochlore-free PMNT starting material for crystal growth using the Columbite process and Pb_3O_4. Pyrochlore-free starting material prevents the crystals from sticking to the walls of the Pt crucibles and thereby prevents some forms of cracking. An another important development was the use of commercial magnesium niobate that reduced the number of processing steps and time by 50%. 2) Measured the liquidus curve in the PMN-PT phase diagram system for the first time. 3) Grew the first large PMN and PMN 10PT single crystals from nonfluxed melts by the Bridgman method during the first year and had their properties measured. These crystals grew along the 111 direction, their fast growth axis and their properties were consistent with literature values, 4) Grew large, transparent one inch diameter boules of PMN-35PT and PMN-32PT crystals using seed crystals for evaluation of compositional and structural uniformity, crystalline defects, etc. Uniform axial and radial composition was found in one cm diameter boules but axial Ti concentration variations were over 10 % in one inch diameter crystals.

Samples have been submitted for property measurements and evaluation to NUWC, Tetrad, Washington State University, Penn State University, Hewlett Packard, Wilcoxon, etc. It was found that the properties of the tetragonal PMNT phase (greater than 35% Ti) were not as good as those for rhombohedral crystals.

INTRODUCTION

This Final Report on ONR Grant # 00014-97-1-1000 covers the period July 30, 1997 to July 31, 2001. The original goal of this program was to the growth of large single crystals of both lead magnesium niobate- lead titanate (PMN-PT) and lead zinc niobate (PZN-PT) solid solutions using the vertical Bridgman and, if necessary, the vertical zone melting methods. Early in the program it was realized that PZNT Bridgman growth and zone melting studies would be too challenging for the time period and level of effort supported, and therefore the program goals were scaled back to concentrate principally on the Bridgman growth of solid solutions in the PMN-PT system.

The initial phase of this program was to test the viability of the Bridgman method for the growth of the lead-based relaxor ferroelectrics. Our previous research on the Bridgman growth of lead barium niobate (PBN) single crystals in sealed platinum crucibles suggested that this technology was useful for materials with high component vapor pressures such as PMN-PT. At the start of this program we had to overcome a few basic obstacles. Most important was that no high temperature PMN-PT phase diagram data was available. These diagrams give information on melting temperatures and segregation behavior as a function of PT concentration. Second there was some concern about the possible concurrent formation of a closely related pyrochlore phase during growth or cooling, and how that would effect the crystallization of the perovskite phase. Finally, large oriented seed crystals were not available. As a result we had to proceed cautiously during the first experiments and decided to start with the growth of pure PMN while we determined some of the thermodynamic properties of the PMN-PT solid solution system.

Using a successful self-seeding technology developed in our laboratory for growing PBN single crystals, and a synthesis method for eliminating the pyrochlore phase from the starting material, high quality PMN single crystals (one cm in diameter) were grown by the Bridgman method for the first time. The process appeared to be quite straightforward. Our conference presentations on the early success of the Bridgman growth of pure PMN at Stanford University persuaded a number of other commercial organizations to pursue this technology for the growth of PMNT. Shortly afterwards success was reported by Stanford and other groups on the growth of the rhombohedral phase of PMN-PT in solid solution concentrations up to about 35% PT. Boule sizes up to one inch in diameter and 4-5 inches in length could be produced.

The limited availability of seed crystals at Stanford was a problem during the course of this program. The grain selection process did not go to completion as readily during the growth of solid solution single crystals. Usually, a few grains aligned along the growth axis persisted to the top of the boule. Therefore scaling up from 1 cm diameter boules with a few grains to a one inch diameter boule was not straightforward. For this purpose tapered crucibles were employed. However,

crucible leaking and the higher crucible costs compared with straight-sided crucibles were inhibiting factors.

Normally solid solution systems like PMN-PT exhibit compositional segregation during growth. The extent depends on the separation of the liquidus and solidus curves, material properties and the growth method used. Unidirectional solidification by the Bridgman method typically leads to an axial variation in composition unless mass transport takes place solely by diffusion. In this case steady state growth of a constant composition is possible. However, buoyancy driven convection is usually present during growth when thermal and/or solutal gradients exist, and this leads to segregation, in particular Ti during the growth of PMNT. Since some PMNT properties change dramatically with Ti concentration, particularly near the morphotropic phase boundary, compositional uniformity is very important.

One cm diameter crystals did not have much axial or radial compositional variations. This was probably due to restricted convection. However, in one inch diameter boules, the compositional variations were significant. Such an eventuality was mentioned in our original proposal and the zone melting method was proposed to solve this problem. Unfortunately time did not permit pursuing this approach in this program, but is being studied in a new follow-on program in collaboration with TRS, Inc.

One of the principal goals of this program was to transfer the technology developed to the industrial sector to enable the routine growth of these materials. This was accomplished via presentations at meetings, in published papers (1) and via consulting activities. The Bridgman method was found to be a relatively simple technique requiring simple furnaces and crucible design, and very little operator attention to run successfully. These advantages make them easy to commercialize. Based on his experience learned in our laboratory, one of our visiting scholars, Dr. Sang-Goo Lee started his own company "Ibule Photonics Co. Ltd in Korea to manufacture these crystals.

During the course of this investigation samples were supplied to a number of groups for property measurements (including Tetrad, Penn State, etc). The properties of most PMNT crystals seems to depend more on the composition, orientation and compositional variations than on other types of crystalline defects. Generally, compositions just below the morphotropic phase boundary (~32%PT) are most desirable for device applications.

This final report will cover various aspects of our research program including starting material preparation, phase diagram studies, growth experiments and property measurements.

BACKGROUND

Relaxor ferroelectrics, such as PMN and PZN, are complex perovskites characterized by a diffuse maximum of dielectric constant associated with a strong frequency dispersion. The relaxor properties can be attributed to complex order-disordered nanostructures and the formation of local polar domains. Solid solutions between a relaxor compound (ex. PMN) and a material like lead titanate (PT), a structurally related ferroelectric compound having long-range order, was expected to combine the advantages of both. Materials such as single crystal PZNT and PMNT have been found to exhibit an extremely large piezoelectric strain and a very high electromechanical coupling factor. The high longitudinal coupling (k_{33}) values (~90%) and piezoelectric coefficients (d_{33} ~ 1500pC/N) reported for these materials (2,3) make them attractive for both actuator and transducer applications.

While the merits of using PMNT and PZNT in single crystal form were clearly evident, systematic studies on their growth and characterization were only in their early stages when this program began. Bonner and Van Uitert (4) were the first to grow single crystals of PMN. They used the Kyropoulos technique (growth on or near a free melt surface), both with and without seeding. The resulting crystals ranged in size from 0.3 to 1.5cm. While the Kyropoulos technique will yield single, oriented crystals, the evaporation some components from the melt surface will limit the crystal size and compositional uniformity.

When the strong interest in relaxor ferroelectric single crystals developed about 10 years ago, crystal growth studies on PMN-PT and PZN-PT became focussed on the flux growth method. To date, PMN, PZN, and PMN- and PZN-PT single crystals have been grown from fluxes between 1150 and 1200°C(5-9). The normal unseeded flux growth method is not an ideal method for the commercial production of large high quality single crystals of these materials. Both lead oxide and boron oxide are very volatile above 1000°C. This effects not only nucleation density and crystal size but also can lead to compositional non-uniformity in the resulting crystals, including flux inclusions and pyrochlore formation. The use Pb_3O_4 to provide extra oxygen to the melt helped suppress pyrochlore formation. Some of these problems can be partially eliminated by sealing the growth crucible. However, this makes it difficult to seed the melt and thereby the produce large oriented crystals.

A clever solution to the problems associated with the normal flux technique, was the introduction of the flux-Bridgman method for the growth of PZNT solid solutions. Using this method with sealed crucibles, a fluxed melt based on PbO, seed crystals and a solid nutrient source to maintain constant composition, Yamashita et al (10) at Toshiba in Japan were able to prepare large uniform single crystal boules of PZNT of commercial quality.

At the beginning of this program, information on the growth of PMNT or PZNT using the normal Bridgman technique (nominally pure melts without a flux) was not available in the literature. The Bridgman growth technique can eliminate most of the problems described above for the flux method by using a sealed crucible and seeding. In addition the growth rates can be significantly faster than with fluxed melts, and inclusions either reduced or eliminated.

This research program was designed to efficiently find the most appropriate parameters for growing large single crystal PMN-PT by the vertical Bridgman. It included a high temperature thermodynamic investigation of the PMN-PT system so as to determine the melting and segregation behavior of the various compositions of interest. The phase relationships found in this part of the program were very helpful in determining the most appropriate melt compositions and processing variables to be used for the synthesis and growth of the desired phases. The initial growth experiments, based on the phase diagrams developed, involved small (1 cm) diameter crucibles. We did a very systematic study using the Bridgman technique to grow both pure PMN and different compositions of its solid solution with PT. The compositions of most interest were those which were nearest the morphotropic phase boundary (MPB) between the rhombohedral perovskite phase and the tetragonal phase where the electromechanical properties are enhanced (3). When an optimal set of conditions was found, the process was scaled up to produce 1 in. diameter, 4in. long boules. Even larger crystals are possible with this crystal growth technology. Careful analysis and property evaluation was used throughout the program to assist with process optimization.

EXPERIMENTAL METHODS

A. Phase Diagram Studies

An understanding of the phase relationships under various conditions of temperature, composition and pressure is vital to the design and control of any crystal growth process. While the low temperature phase diagram for PMN-PT was more or less well known, reliable thermodynamic data on the melting behavior, phase stability and segregation behavior of PMNT solid solutions at high temperatures were not available in the literature at the beginning of this program. Differential thermal analysis (DTA) was, therefore, used to investigate the melting behavior of (1-x)PMN-(x)PT as a function of mole fraction of PT. Ceramic charges of various compositions, (x = 0, 0.10, 0.20, 0.25, 0.30, 0.35, 0.40 and 1.0), were sealed in small platinum

DTA capsules, and analysis was carried out in a TA Instruments DTA using alumina powder as a reference material. Figure 1(a) and Figure 1(b) show the heating and cooling curves from DTA runs on two representative compositions. In the 0.9PMN-0.1 PT sample, Fig 1(a), the onset of melting at 1321°C (lower curve) and the onset of freezing (upper curve) can be seen to coincide, indicating that supercooling is very small for this composition. In the 0.65PMN-0.35PT sample, however, a significant amount of supercooling (ΔT= 25°C) can be detected, with the onset of melting at 1296°C. The melting temperatures of pure PMN and pure PT were found to be 1320°C and 1285°C respectively. Between these end members, the melting temperatures decreased nearly monotonically as the mole fraction of PT increased from 0-100%. The liquidus curve obtained from this data is shown in Figure 2. There is a slope change in this curve at 20% PT giving some indication that a small maxima may be present. This would indicate a congruent composition at that point. While there was some DTA data giving information on the solidus curve, a more realistic picture of the phase diagram was be obtained from phase segregation information obtained from crystal growth experiments.

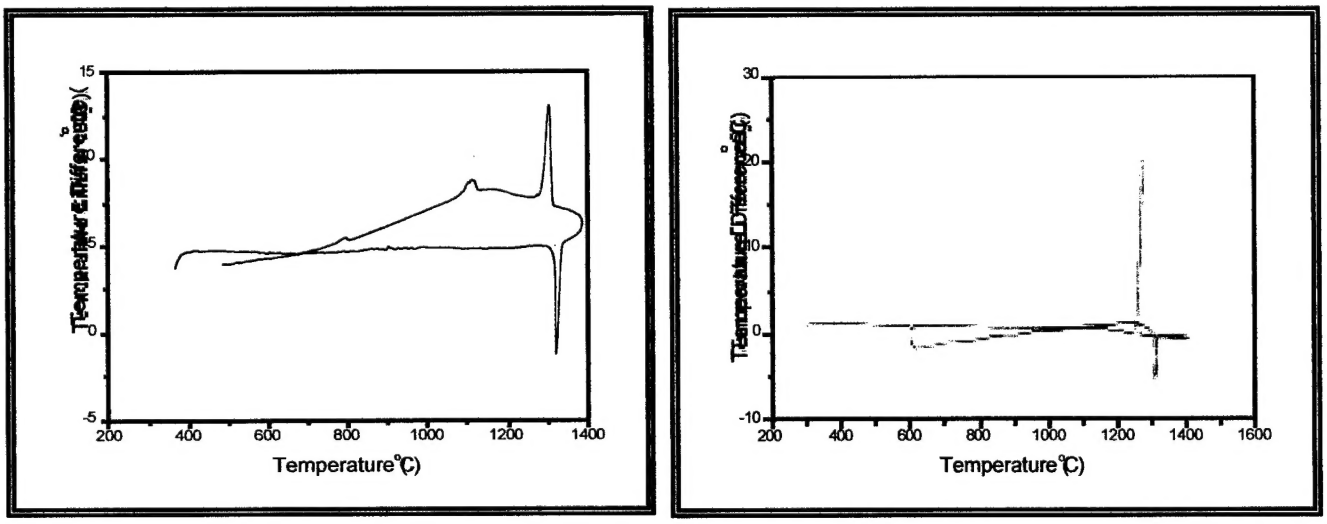

(a) (b)

Figure 1. Heating and cooling DTA curves for (a) 0.9PMN-0.1 PT and (b) 0.65PMN-0.35PT

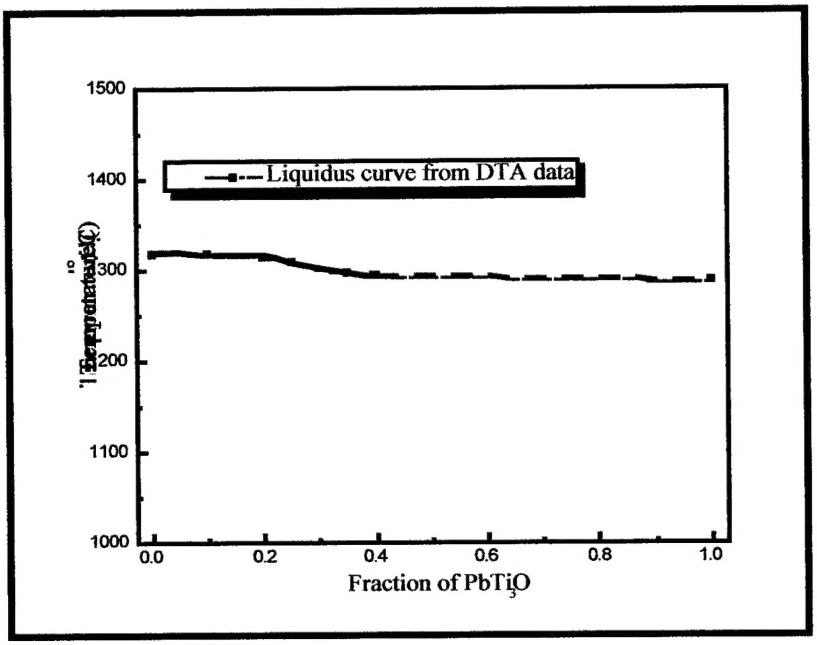

Figure 2. PMN-PT phase diagram

A> B.Material Synthesis

In early work on the preparation of PMN and PMNT ceramics, viable techniques were developed for the synthesis of these compounds. The difficulty of reacting a low melting volatile compound such as PbO with a refractory materials such as MgO, and the stable formation of a neighboring phase (pyrochlore) were major problems to be overcome.

In Bridgman growth it is possible to charge the crucible with the component oxides and, via various intermediate reactions, obtain a homogeneous melt. In some cases it is hard to control the reaction because 1) the lower melting materials melt will usually migrate downward toward the bottom of the crucible before reacting with the higher melting components and 2) the lighter, unreacted components can also float on top of the melt making it difficult for the reaction to go to completion. For example MgO is not only more refractory that PbO it is also much lighter. We therefore chose to presyntheisze our charge to avoid these problems and took advantage of earlier work on the preparation of Pyrochlore-free starting material.

In this program PMN charges were prepared by using the 2 step columbite precursor method (11).

Step 1: $MgO+Nb_2O_5 \rightarrow MgNb_2O_6$

Step 2: (a) $3Pb0 + MgNb_2O_6 \rightarrow 3\ PMN$

(b) $Pb_30_4 + MgNb_2O_6 \rightarrow 3PMN + 1/2O_2$

This method makes it easier to get the reaction to go to completion compared to a one step calcination using only the binary oxides. In this method, stoichiometric amounts of MgO and Nb_2O_5 were first ball milled in ethyl alcohol, dried in oven at 150-200°F for 20 hrs. and then fired at 1100°C for 7 hrs to form $MgNb_2O_6$. This was then reacted with PbO at 900°C for 4 hrs to form PMN. The high temperature processing was done in platinum crucibles. In order to synthesize PMN-PT an additional step is required wherein PMN was reacted with $PbTiO_3$ at 900°C for 4 hrs. The calcined materials were then ground using a mortar and pestle. During the course of this program a reliable commercial source of $MgNb_2O_6$ became available and this was used in subsequent experiments (eliminating step 1) without decreasing the quality of the resulting product.

Using step 2a, a small amount of residual pyrochlore was found in the charge material as seen in Figure 3a. This was not a significant problem in Bridgman growth as most of this phase migrated to the top of the boule where it was benign. It is not clear whether this happens during melting or by segregation during growth. However, a small thin layer

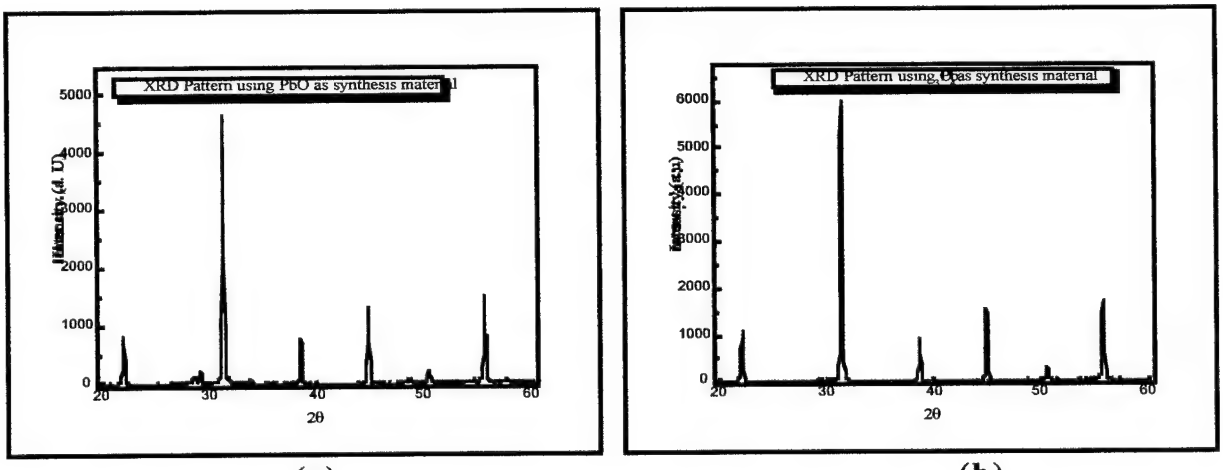

(a) **(b)**

Figure 3. X-ray diffraction patterns of charge material made with a) PbO and b) Pb_3O_4

was also found in patches between the crucible wall and the boule and led to some sticking to the crucible wall. This caused some minor pullouts on the boule surface making it more difficult to

remove the boule from the crucible. The use of Pb_3O_4 instead of PbO (as shown in Step 2b) was found to inhibit the formation of the parasitic pyrochlore phase (11), as shown in the x-ray powder diffraction pattern in Fig 3b. Since Pb_3O_4 is unstable at elevated temperatures, it dissociates during calcining ($Pb_3O_4 \rightarrow PbO + O_2$) and thereby introduces extra oxygen into the system. This seems to retard the formation free lead in the charge via the reduction of PbO. The presence of Pb can cause Pt crucibles to leak since it is known to attack the grain boundaries.

C. Crystal Growth

1. Crucible preparation

Crucible preparation is very important in the Bridgman growth of PMNT since the leaking problem can completely ruin an experiment (if the leak is near the bottom the entire charge can leak out in a very short time). It has been well known for over 40 years that PbO-containing melts can attack Pt at elevated temperatures. Figure 4 shows a crucible that leaked during a growth run. Sometimes the leaks developed at defects in the welds and sometimes through the crucible walls, particularly if the wall thickness was too thin. Sometimes some small melt patches appeared on the outside of the crucible, but this did not seem to affect the crystal inside.

During this program different crucible strategies were tried, including home made and commercial, tapered and straight sided, and varying wall thickness. Commercial tapered crucibles with 25.4 mm at the full diameter (like that shown in Figure 4) were, in general, not very successful. Sixteen tapered crucibles obtained commercially had to be sent back as they were found to leak extensively due to thin spots (0.17mm) and surface defects caused by the manufacturing method. Smooth, rolled Pt foil, 0.4 mm thick and welded in our shop along the side and bottom gave the best results. Both the 1 cm and 1 inch diameter crucibles were about 150 mm in length. While the boules usually do not stick to the crucibles they do not slide out after the welded top is removed, and so the crucible has to be carefully cut away. It is very unlikely that Pt crucibles could be reused in any event, since at these very high temperatures grain growth in the metal during the first run would probably lead to serious leaking via the grain boundaries during the next run.

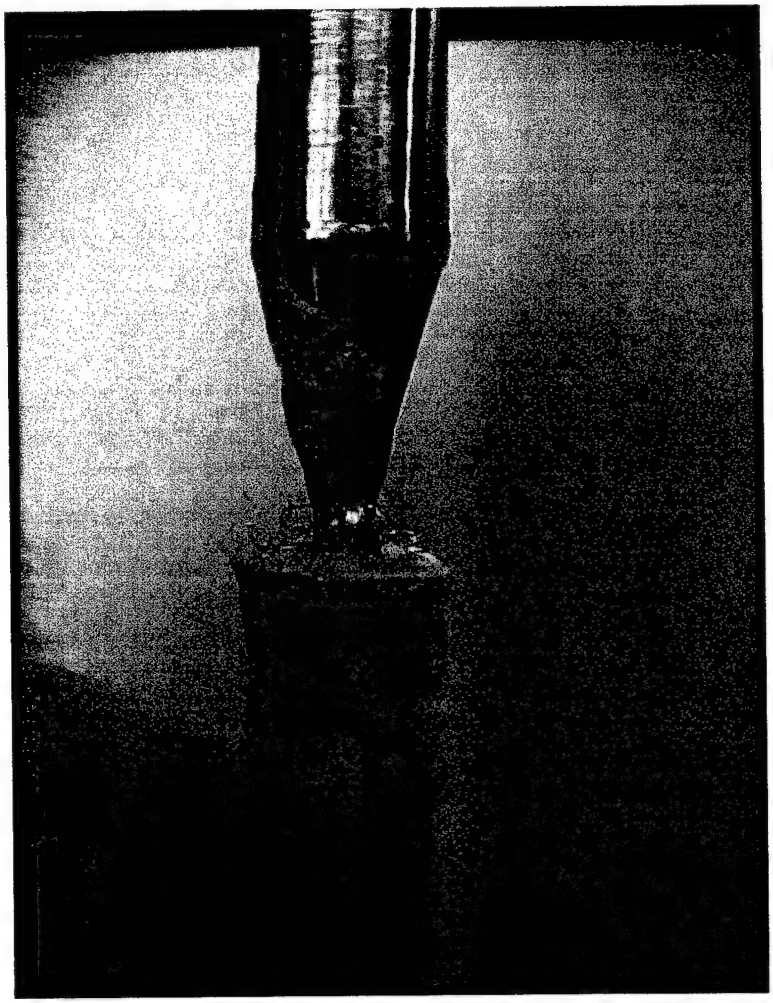

Figure 4. PMNT melt that leaked out of a commercial tapered Pt crucible onto the ceramic crucible holder during a growth experiment.

2. Growth Furnace

Two commercial, high temperature cylindrical furnaces were used in our laboratory for the growth of PMN and PMNT single crystals. One contained four large U-shaped $MoSi_2$ heating elements and the other eight smaller ones. A schematic of the furnaces is given in Figure 5, along with an example of a tapered crucible and the crucible support tube. The furnace systems were set-up to provide an axial furnace temperature gradient of about 25-30°C/cm. The maximum furnace temperature was set so as not exceed 1400°C. (The higher the temperature the greater the reactivity of Pt and PbO). A typical measured profile is shown in figure 6, along with a schematic of a flat bottom crucible packed with a powder charge at various stages of a growth run. Several thermocouples (usually 4) were welded on the side of the crucible in the seed region to control the position of the initial growth interface. The temperature needed for each composition was determined from the phase diagram shown in Figure 2.

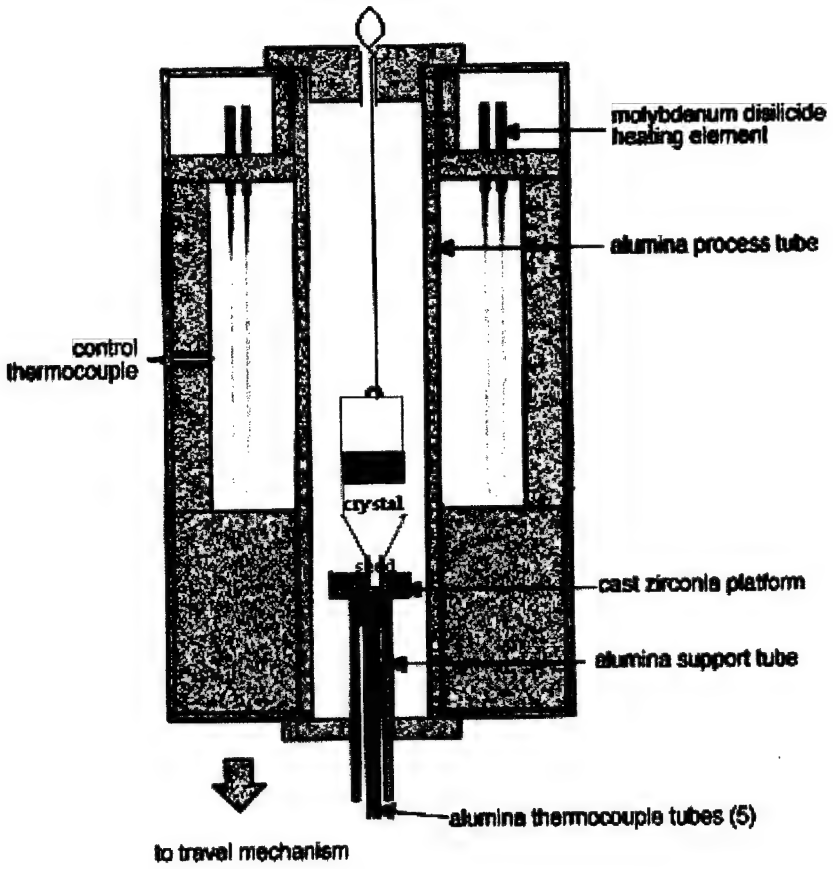

Figure 5. Bridgman growth furnace.

3. Crystal Growth

In the Bridgman method the crucible can either be moved downward or the furnace moved upward to initiate unidirectional solidification. One of our furnaces translated the furnace, the other the crucible. Different furnace or crucible moving rates (which are often different than the actual growth rates) were studied, but 0.8-1 mm/hr were the most often used. Seeding was initially accomplished with packed powders, which relies on aniostropic grain growth and initial grain alignment to reduce the number of grains and increase their size (see Figure 6). Then, in an iterative process, these large grains are used as seeds until the number of grains are reduced to a

single crystal. This technique worked very well for our previous studies of PBN crystal growth and also for pure PMN. However grain selection was poor with the addition of morphotropic quantities of PT, and several large grains of close alignment propagated along the growth direction.

In this research program we started with 1 cm diameter crucibles and afterwards demonstrated that large 1 inch diameter 5 inch long crystals could be grown rather easily. The main requirement in our studies was the availability of a good single crystal seed. Without the use of seed crystals it is difficult to control the growth orientation of the boule. The fast growth direction for PMNT is normal to the {111} and so unseeded boules usually grow close to this axis, but may be up to 30° off.

After growth the crystals are cooled slowly to room temperature, with particular care in the 200° C to room temperature range where the material undergoes a phase transition. The crucible must be removed by cutting it away from the boule from the top downward. In most cases the crystal surfaces are smooth and shiny and the grain structure in the platinum crucible can be seen imprinted on the boule surface.

Figure 6. Furnace temperature profile and a schematic of a self-seeded growth experiment use a using a powdered charge and only partial melting. The crucible on the right shows the partially melted charge and the one on the left after some of the melt has crystallized.

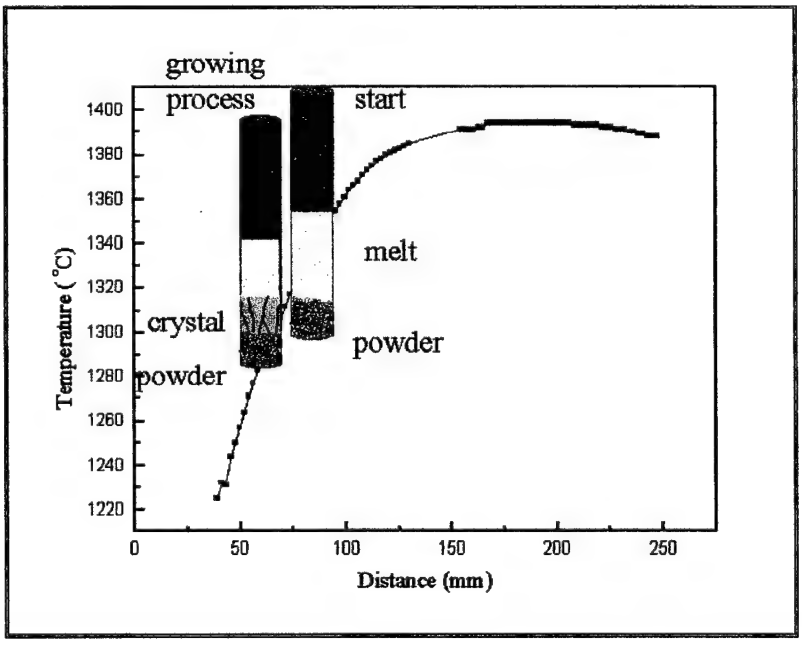

It is possible to grow single crystal boules without a seed by completely melting the charge. In one case a long thin capillary region is attached to the bottom of the crucible and the whole charge melted. Solidification inside the capillary is contained in a small area and, therefore, fewer grains are present, favoring good grain selection. However, if the crucible leaks in this region all the melt will flow out (see Figure 4). Some researchers found that a crucible with a shallow-tapered bottom with a large included angle could be also used to create a large single crystal boule. This requires the melt to have good nucleation characteristics, i.e. a low nucleation density and low supercooling. Severe melt loss will also occur if the crucible leaks at or near the bottom.

D. Crystal Characterization

The boules and samples cut from boules were first studied by optical microscopy. Usually the top and bottom slices were assessed first. The back reflection Laue technique was used to identify the growth direction, and also to orient samples for further analysis. Powder X-ray diffractometry was used to identify phases in the resulting material and electron probe microanalysis to determine the chemical composition of the boules in both the radial and axial directions. Light scattering tomography was used to study domain structure and defects in PMNT crystals. Most ferroelectric measurements were made elsewhere, for example via Dr. Eagle Park at Penn State.

RESULTS AND DISCUSSION

A. Pure PMN

Pure PMN single crystals were obtained in a two step Bridgman growth process First we used packed powder, partial melting and unidirectional solidification in the Bridgman crucible to get a boule which had much fewer, larger grains than the starting powder. Then, using a section of this boule as a seed in the next growth run, we were able to produce a single crystal boule. This work was reported by our group in 1999 in Applied Physics Letters (1). This was the first reported use of the Bridgman method for the growth of any PMN material . A slice from a 4 inch long, one cm diameter single crystal is shown in Figure 7. The color of these crystals varied from pale yellow to greenish yellow.

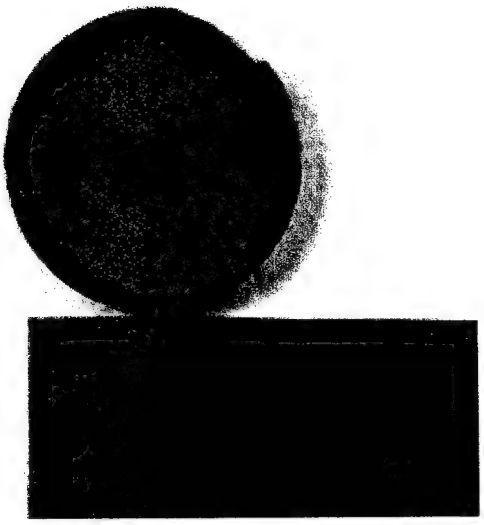

Figure 7. Slice from a 1 cm diameter single crystal boule of pure PMN.

The physical properties were measured along the <111> growth direction. The variation of dielectric constant and dielectric loss with temperature for various frequencies can be seen in fig. 8 While a typical polarization and strain curve obtained for relaxor ferroelectrics is shown in figure 9.

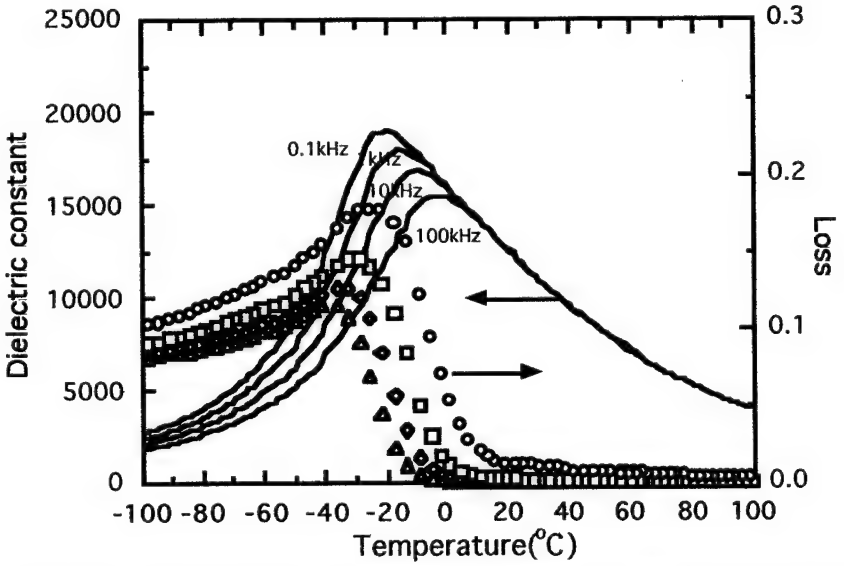

Figure 8. Dielectric Constant and Loss as a function of temperature for pure PMN crystal.

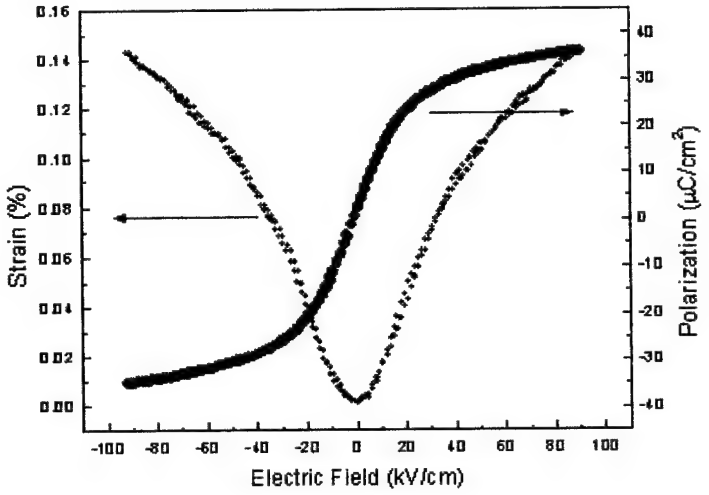

Figure 9. Strain and polarization behavior for PMN single crystal

B>

C> B. PMN-PT

1. Composition and Structure

Several different PMN-PT compositions were grown during the course of this program, including 10, 25, 32 and 35 % PT. The first Bridgman growth experiment of a PMNT solid solution was carried in a manner similar to pure PMN growth. It was done in a flat bottom, 1 cm diameter sealed Pt crucible with seeding off packed powder in a partially melted charge having a composition of 10% PT. The crystals were very transparent with a pale yellow color, as shown in Figure 10. Grain selection was favorable and a large single crystal region with only two smaller grains resulted. This rhombohedral material has a high optical transparency because at 10% PT the ferroelectric domain boundaries do not scatter light. The grain boundaries, however, can be seen clearly. As we will see later, grain boundary and domain scattering are much more intense for compositions near the morphotropic phase boundary.

Since there was only peripheral interest in PMN-10PT crystals, we immediately started to grow solid solutions close to the morphotropic phase boundary (MPB), at first with a 35 % PT charge. Grain selection was very poor in self-seeded experiments using PMN-35PT powder. Fortunately PMN-10PT has a higher melting temperature than PMN-35PT and, therefore, this makes it possible to use it as a seed. So we prepared seed crystals from one of the 1 cm diameter 10%PT boules. Using this seed we were able to grow a 35% boule with reasonably uniform

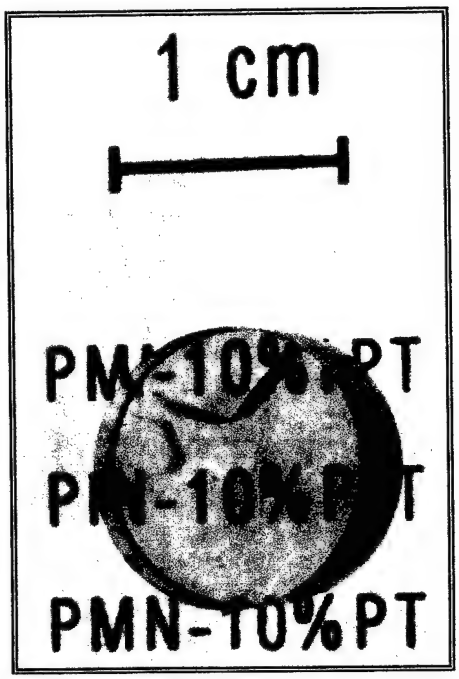

Figure 10. Cross-sectional polished slice from a 1 cm diameter 10% PMNT boule (#16).

composition. This is shown in Figure 11. Note that the Ti concentration in the main section of the boule is 35%. There is some intermixing between the 35%Ti melt and the 10%Ti seed, which is partially melted during the seeding process. Note the corresponding decrease in Nb content in this region as the Ti content increases.

Unfortunately the seed used was not completely single, having 3 or 4 grains, and they propagated up the boule without much change in size. This means that the alignment of these grains was similar, and close to the <111> fast growth axis. Several sections of this boule were cut from the 35% PT region and used to grow a boule of the same composition. This boule is shown in the photograph in Figure 12. The cut section on the left shows the grain structure of the seed and the one on the right the grain structure at the top of the boule. Note that there was not much change in either the number or size of the single crystal regions. The boule, while generally transparent throughout, contained a cloudy section in the first few cm of growth and a clear region afterward (as indicated in the photograph in Figure 12). Although compositional analysis was not made on this boule it is probable that the cloudy region contains both tetragonal and

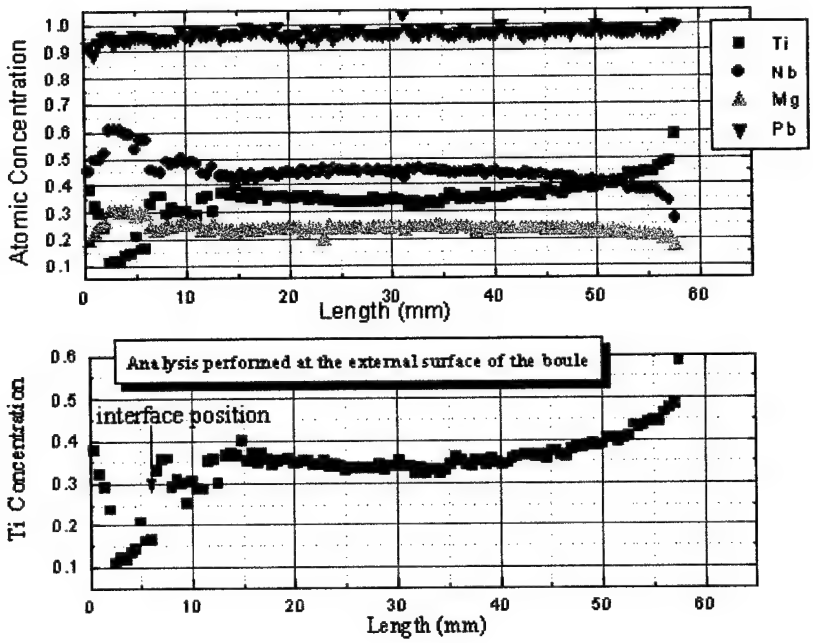

Figure 11. Axial composition profiles of a PMN-35PT 1 cm diameter boule grown from a 10% seed crystal. The distribution of all the components is given in the top figure while a more expanded view of just the Ti segregation is the lower figure. The composition of Ti can be seen to rise from 10% at the start of the run to 35% and then level out in the center section of the boule.

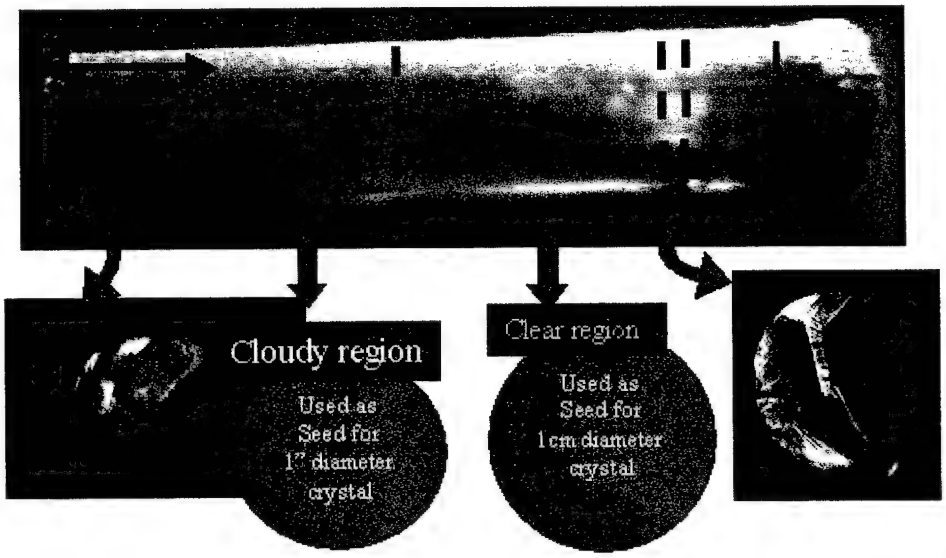

Figure 12. One cm diameter boule (#21) grown from a 35% seed crystal. Various seeds were cut and used to grow 1 inch diameter boules

rhombohedral regions. This is consistent with Kelly et al (12) who report that ceramic samples with compositions in the range 27% PT to 60% PT contained varying quantities of both phases.

A seed crystal from the cloudy section of boule # 21 above was used to grow a one inch diameter crystal. A tapered crucible with a seed pocket, like that shown in Figure 4, was used in this experiment. The seed was ground to fit the seed pocket. In the first such experiment a 1 inch diameter and 50 – 60 cm long boules was produced, an example of which is shown in Figure 13. Since the seed contained a few misoriented grains, the larger boule also had a remarkably similar grain structure. However, because of the larger diameter of the crucible, these single crystal regions were much larger. It is clear that if a single crystal seed had been available, a single crystal boule would have resulted. Boule 26 shown in Figure 13 was cut and oriented. From this some large single crystal regions were obtained one of which is shown in Figure 14. Some material was used for seeds and the section in figure 14 for was used to prepare (001) plates for poling studies and property measurements.

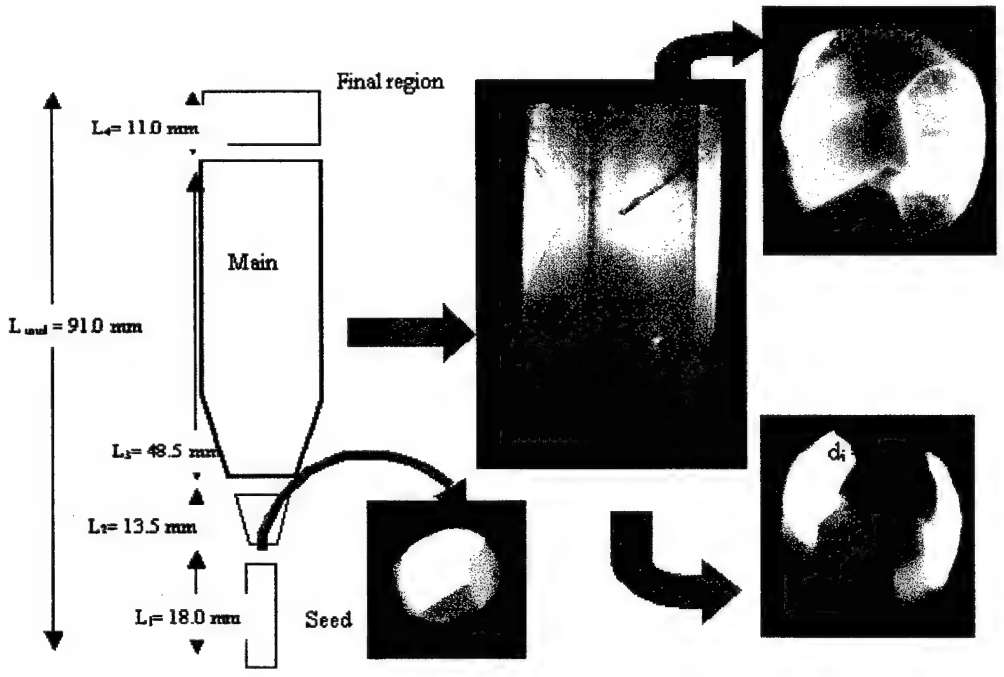

Figure 13. Seeding a 1 inch diameter boule using a 1 cm diameter seed having several grains. Even though the grains propagate into the expanded diameter the resulting single crystal regions were very large.

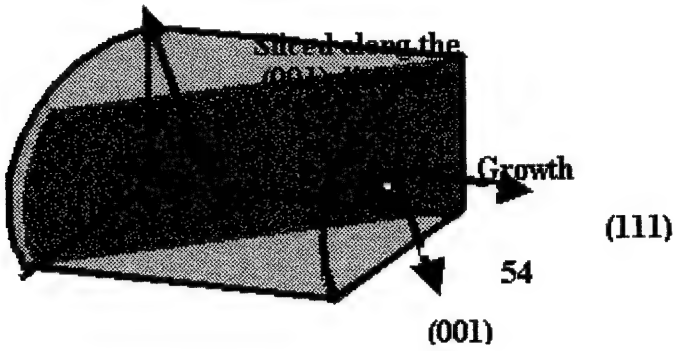

Figure 14. Schematic section of a portion of the above boule showing the orientation of the (111) and (001) directions. Many (001) plates were cut from this sample.

In this large 1 inch diameter boule, we found that the composition was much less uniform along the growth direction than the 1 cm diameter crystals. The variation of Ti concentration with length is shown in Figure 15, along with part of the polished longitudinal slice from which the compositional data was obtained using EPMA analysis. In this section of the boule the composition varied from 30%-40% Ti, even though the melt composition was 35%. This segregation behavior clearly shows that PMNT-35 is not congruently melting, in agreement with the expected solidification behavior of solid solutions.

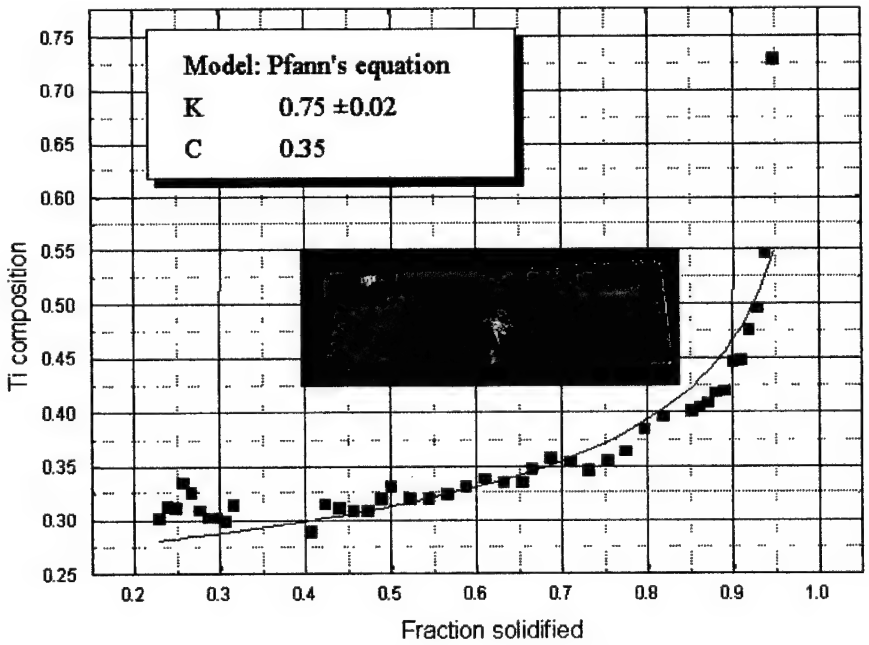

Figure15. Plot of Ti concentration versus fraction solidified for a longitudinal slice of boule # 26 having a charge composition of PMN-35PT (part of which is shown in inset). From this curve the segregation coefficient for Ti was calculated (red Line) to be 0.75.

The variation in composition with distance along the boule can also be seen in the x-ray diffraction data of figure 16. The two powder diffraction patterns were obtained from samples taken from the top and bottom of boule no. 26. They show that in the early part of growth, the crystal had the rhombohedral structure (red curve) while near the top it was tetragonal (see the line splitting at higher values of 2 theta showing both a and c reflections). This behavior is what one would expect for compositions greater and less than the morphotropic composition 35% PT, (in this case the samples were < 30% PT and >40% PT).

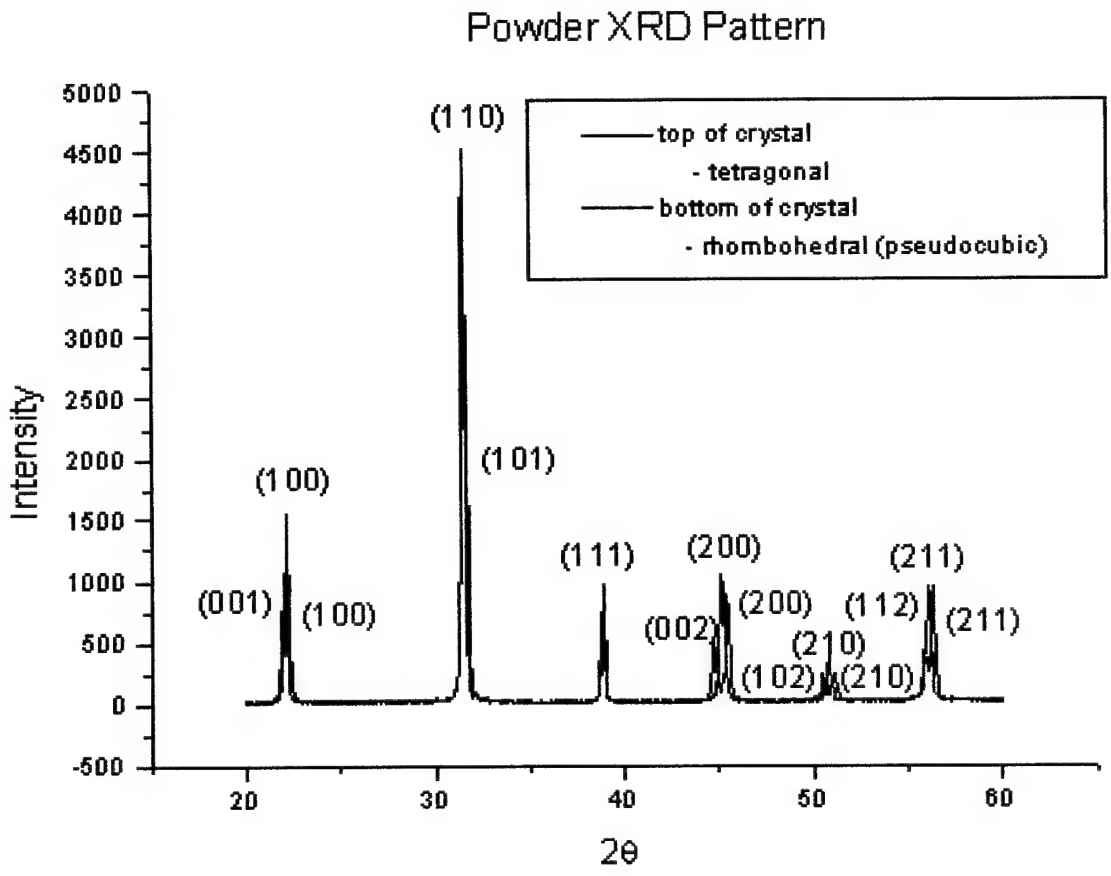

Figure 16. Powder x-ray diffraction data obtained for samples taken from near the bottom and top of boule No. 26.

The compositional variations can also be seen in the dielectric constant data as a function of distance along the boule. Figure 17 shows such data for some samples from the tetragonal region.

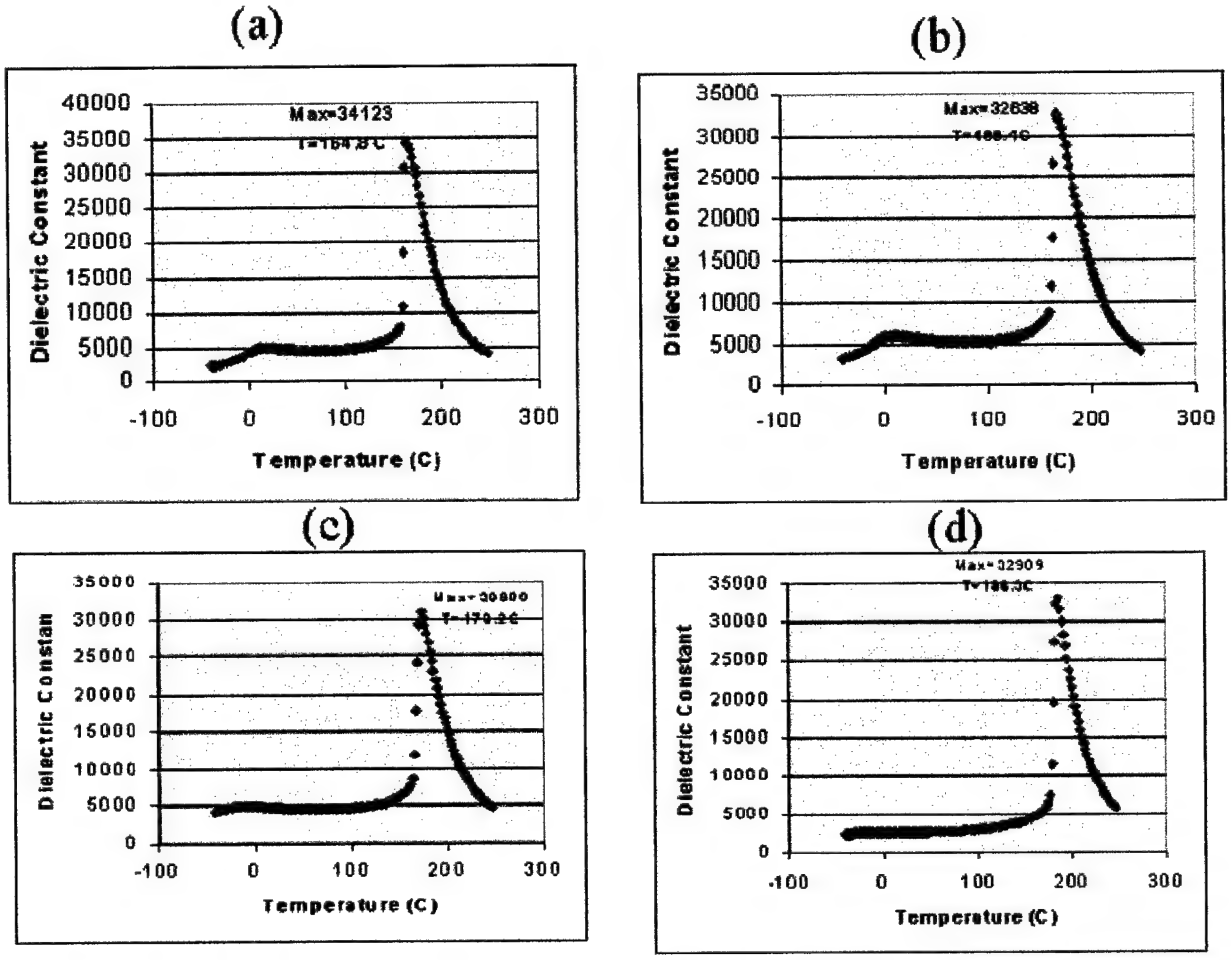

Figure 17. The graphs of dielectric constant as a function of temperature were taken from samples with compositions just above the MPB, i.e. in the tetragonal region. The samples were oriented in the [001] direction. From (a) to (d) the composition increases in Ti concentration and this is seen in the shift of the dielectric anomaly to higher temperatures.

The variation in axial composition in Bridgman growth depends on the details of the mass transport in the system, which in turn, depends on convection the melt (usually buoyancy-driven). The uniform axial composition in the smaller diameter PMNT boules behaves like diffusion-controlled growth where convection and melt mixing/homogenization are negligible. Certainly convection is restricted in the small diameter ampoules, however it is unlikely that

convection is zero. It is more probable that the net convection in terms of moving nutrient to the growth interface is negligible. In the large 1 inch diameter convection is more of a cooperative effect and this leads to segregation behavior more in line with mathematical models incorporating complete mixing. The corresponding compositional profile for the 1 inch diameter boule can be fit by the equation

$$C_s = kC_o\,(1\text{-}g)^{k-1},$$

Where C_s is the concentration of solute (in the present case Ti), C_o is the initial concentration (Ti = 35%), g is the fraction solidified and k is the segregation coefficient. This equation fits the data curve shown in Figure 15 (red line) for a k value of 0.75.

Based on this type of data we could more accurately determine the solidus curve for the PMN-PT phase diagram than from DTA data. We know for example that if we start with a 35% PT concentration and the first solid to form is say 30%, then at that temperature the solidus curve coincides with 30% PT. This can be seen in the phase diagram construct in Figure 18.

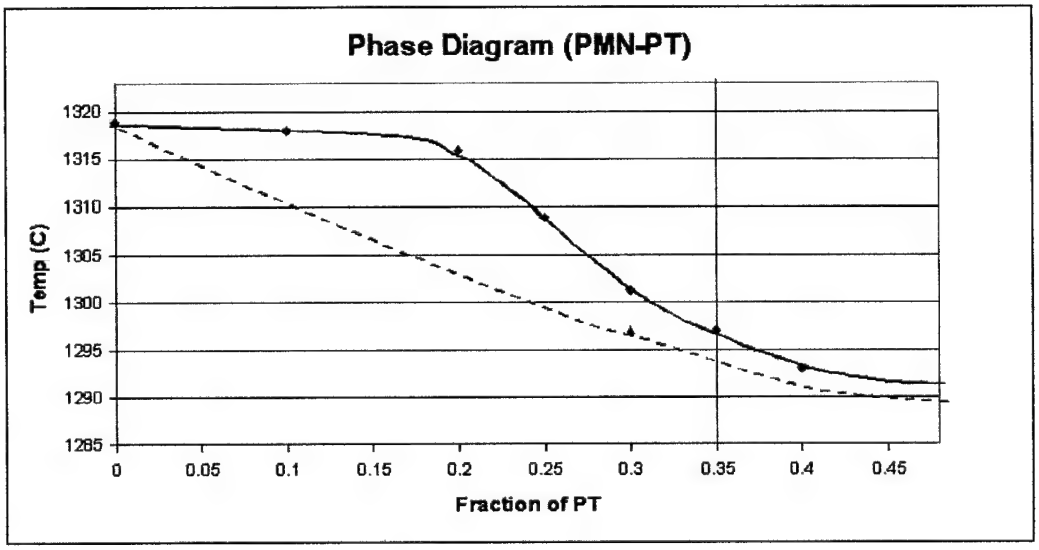

Figure 18. An illustration of how the solidus curve (dashed) could be constructed from solidification data. In this case we have only one point from a 35% PT melt yielding a solid with about 30% PT. To determine the actual solidus curve, several different melt compositions would have to be solidified by the Bridgman method, and the initial solid composition measured along with compositional variations along the boule axis..

The liquidus curve in Figure 18, the solid line, is from DTA data and the dashed line just a two point approximation of the solidus curve. To actually determine the shape of the solidus curve, however, boules would have to be grown from melts having a number of different compositions between 0% and 100% PT, and then the compositions of the resulting boules analyzed.

One of the more interesting questions in the growth of PMN-PT solid solutions is what phases are present in unpoled boules of varying composition near on the MPB. The usual low temperature phase diagram indicated that the MPB is a line separating two single phase regions. If this is a pseudo-binary phase diagram, then this violates the phase rule, which requires a two phase region in-between which contains both the rhombohedral and tetragonal phases. In this region the two phases would have different compositions at a given temperature, one being richer in PT than the other. In the PMN-PT system, the amount of rhombohedral phase decreases with increase in PT content until we are left with only the tetragonal phase. This effect was discovered by Kelly et al (12) who's data are given in Table 1 below, along with the corresponding relationship between physical properties and composition.

Table 1. Structure, composition and properties as a function of PT concentration in ceramic samples (Kelly et al (12))

Composition	Structure (%)		Dielectric constant K, at room temperature	Piezoelectric charging coefficient, d_{33}, (pC N)	Planar coupling coefficient, k_p (%)	Thickness Coupling coefficient, k_t (%)
	Rhombohedral	Tetragonal				
0.80PMN-0.20PT	100	0	2464	230	*	*
0.76PMN-0.24PT	100	0	2562	240	.20	*
0.74PMN-0.26PT	100	0	2459	240	.25	*
0.72PMN-0.28PT	69	31	2339	320	.51	.38
0.70PMN-0.30PT	63	37	2950	450	.55	.41
0.69PMN-0.31PT	60	40	3661	570	.57	.44
0.68PMN-0.32PT	57	43	3738	590	.62	.43
0.67PMN-0.33PT	55	45	3717	640	.61	.43
0.66PMN-0.34PT	49	51	4360	670	.62	.42
0.655PMN-0.345PT	49	51	5419	720	.62	.45
0.65PMN-0.35PT	48	52	5229	700	.61	.44
0.645PMN-0.355PT	46	54	5128	650	.60	.42
0.64PMN-0.36PT	40	60	4684	585	.59	.38
0.62PMN-0.38PT	35	65	3525	465	.32	.15
0.60PMN-0.40PT	28	72	2692	370	.22	.10
0.55PMN-0.45PT	6	94	1556	240	.15	<.10
0.50PMN-0.50PT	7	93	1085	160	<.10	<.10
0.45PMN-0.55PT	5	95	846	80	<.10	*
0.40PMN-0.60PT	2	98	681	50	*	*
0.35PMN-0.65PT	0	100	584	<50	*	*
0.30PMN-0.70PT	0	100	529	<50	*	*

The ceramic samples used in these experiments were produced under near equilibrium conditions, and one can clearly see that there is a large two phase region beginning at >26%PT and ending at > 60% PT and that the percentage of rhombohedral phase decreases as the PT content increases. While these phases exist in ceramic samples produced by calcining and/or sintering, it was not obvious whether they would form on cooling after Bridgman single crystal growth. So the question was whether boules grown from melt compositions in the range 26 to 60% PT would contain two phase regions?

To look at this issue, a grain in the middle of boule No. 26 was cut into slices along the growth axis. These slices were then ground into a powder for x-ray diffraction analysis. The range of compositions in these sample was between approximately 31% PT to 40% PT. The x-ray results for three slices, two from each end of this section and one from the middle are shown in Figure 19.

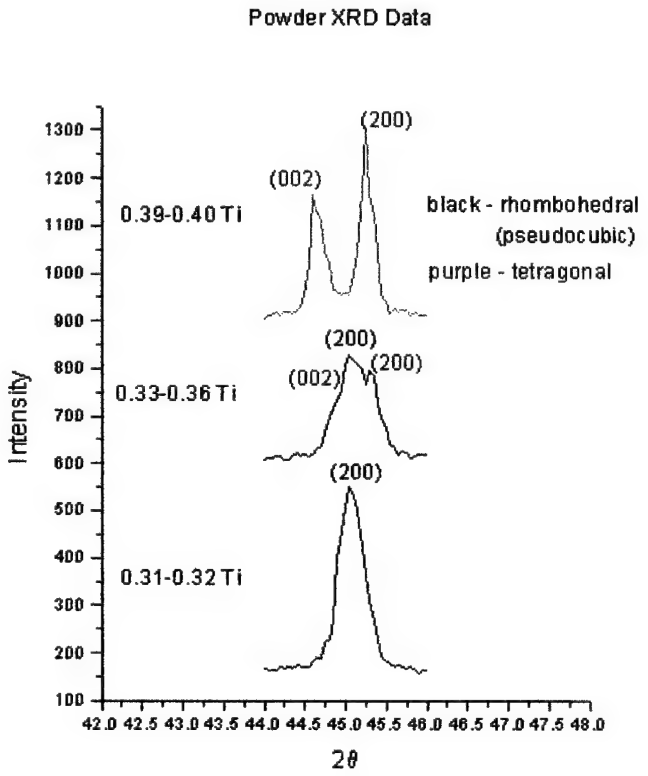

Figure 19. X-ray diffraction data for three sections of boule # 26 having compositions in the 31-40% PT range. The lower curve has the lowest PT composition and the upper curve the highest. Notice that the single rhombohedral (pseudo-cubic) peak splits into two at the higher PT content, indicating the transition to the tetragonal phase. The middle peak contains all three peaks.

The lower curve shows a single, somewhat broad peak centered on the (200) of the rhombohedral phase. The upper curve shows the splitting of the rhombohedral (200) into both the (200) and (002) characteristic of the tetragonal phase. The middle slice is significantly broader than the other two, and one can see both sets of peaks indicting the presence of both the rhombohedral and tetragonal phases. This was also confirmed by Ye et al (9) using optical microscopy.

According to Kelly et al's (12) data, the two phase region should be present in all the samples shown in Figure 19. In fact they should exist in roughly equal amounts. It is possible that the melt growth gives a different result than ceramic processing, since the cooling rates are different. Rapid cooling versus slow cooling (as in the crystal growth runs) could quench in the high temperature phase distribution. This is an area worth exploring through the solidification of different compositions further away from the MPB and annealing and quenching experiments.

2. Optical Properties and Poling

While pure PMN and PMN-10PT samples were generally clear with good optical transparency, samples cut and polished from near MPB compositions had considerable light scattering depending on the exact composition. The transparency varied along the length of all the boules grown with nominal melt compositions near 35% PT. In Figures 15, the inset photograph of a transverse slice of boule #26 along the growth axis shows two types of scattering. At the lower PT compositions (on the left) one sees a cloudy region with scattering from the boundaries of smaller ferroelectric domains, and possibly the boundaries between two phases. In the upper region (on the right) where the tetragonal phase dominates, the crystal has large clear regions interspersed with twins and/or larger ferroelectric domain structures.

Figure 20 shows photographs of a (001) slice taken from the upper part of boule # 26 having a measured composition of 32%PT (rhombohedral side of the MPB). This sample was 1 cm long, 0.5 cm wide and 0.6 mm thick. The photographs on the left are for unpoled samples in reflected (upper) and transmitted light with polarizers crossed (lower). The reflected light sample has a light orange/yellow to brown coloration and is opaque to translucent with internal structure

scattering light. Again this scattering may come from domain walls or phase boundaries. In transmitted light and under crossed polarizers the sample is still translucent. When the sample was poled the transparency improved dramatically as shown in the upper right photograph and all the structure seems to disappear. However, under cross polarizers strain birefringence is seen, particularly along the edges and the lower left side where a grain boundary can be seen.

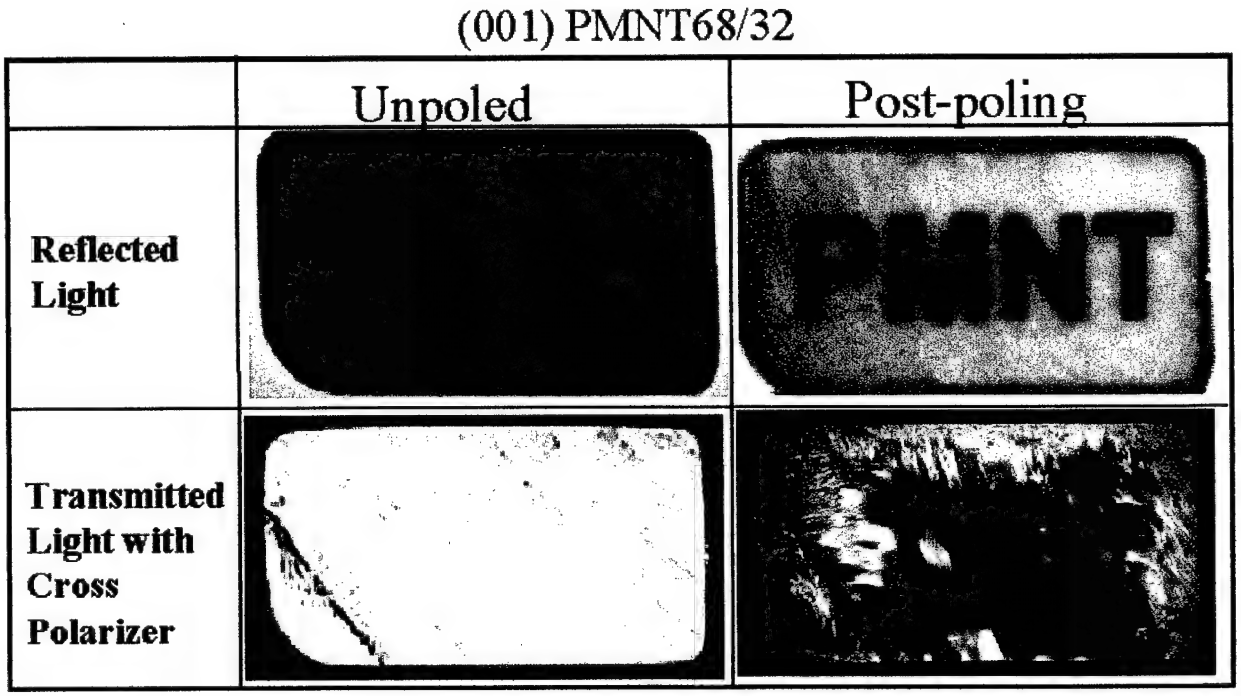

Figure 20. A PMN-32%PT slice under various lighting conditions. After poling the internal structure disappears making the crystal transparent.

The usual explanation for the disappearance of scattering centers under these conditions would be the conversion of the multidomain material to a single domain, hence a reduction in the scattering from domain walls. However, we have evidence that the smaller boundaries from the two coexisting phases also disappear and should reduce the light scattering as well. In Figure 21 theta-omega scans of a (001) oriented single crystal sample containing 32% PT are shown both before (b) and after (c) poling. For comparison, powder XRD patterns of the (200) rhombohedral and tetragonal peaks are given in Figure 21a. It can be seen from Figure 21b that before poling, the θ-ω scan contains three peaks, indicating that both of the above phases are present in this

sample. After poling, however, only a single peak is left (Figure 21c). This reflection is characteristic of the rhombohedral phase. This is in agreement with the usual MPB diagram where a sample containing 32%PT should have only the rhombohedral structure. This suggests that the homogeneity range (26-60% PT) reported by Kelly et al (12) only applies for unpoled material. It must be concluded, therefore, that in the presence of an electric field, the width of the homogeneity region must decrease dramatically, leading to the suggestion that the electric field, like temperature and pressure, is a state variable in this system.

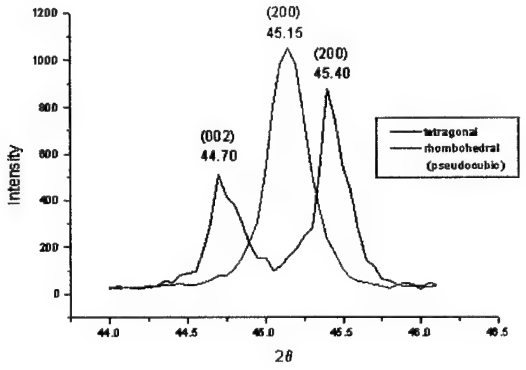

(a)

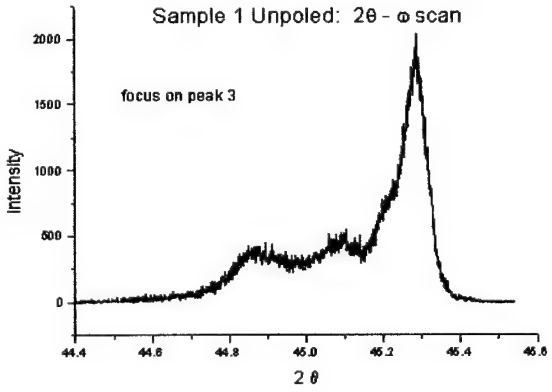

(b)

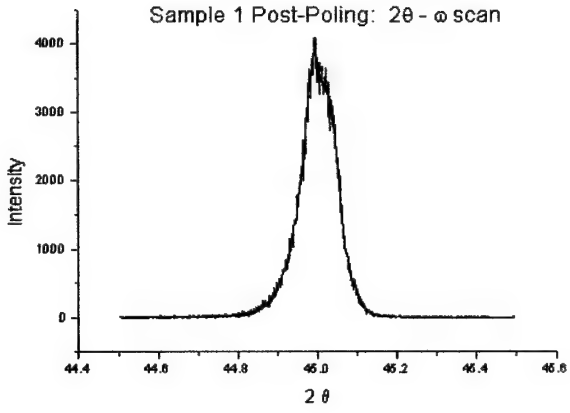

(c)

Figure 21. Theta-omega scans of a (001) oriented PMN-32%PT single crystal sample both before (b) and after poling (c). For comparison an XRD powder pattern (a) is included showing the positions and number of peaks for both the comparable rhombohedral and tetragonal phases.

3. Inclusions/ Grain Boundary Segregation

Flux grown crystals often show the presence of inclusions. These inclusions are usually due to entrapped solvent. One of the virtues of growing from nominally pure melts by a technique such as the Bridgman method is that the solvent inclusions are not present. However, in solid solutions, the crystal composition can differ, sometimes significantly, from the melt composition. The rejected components at the growth interface become, in effect, a solvent phase, inhibiting nutrient from reaching the growth interface. The net result could be the same as growing from a normal solution leading to inclusion formation. A similar situation can develop if the impurity concentration is too high. If the segregation coefficient is very low, the impurity(ies) can build up at the interface and become trapped in the crystal as inclusions.

The presence of inclusions in Bridgman grown PMNT so far has not been a significant problem. We did detect, however, the presence of a few inclusions isolated at grain boundaries as seen in Figure 22. Since inclusions were not seen in the matrix the causes of the inclusions at the grain boundaries may be a special case.

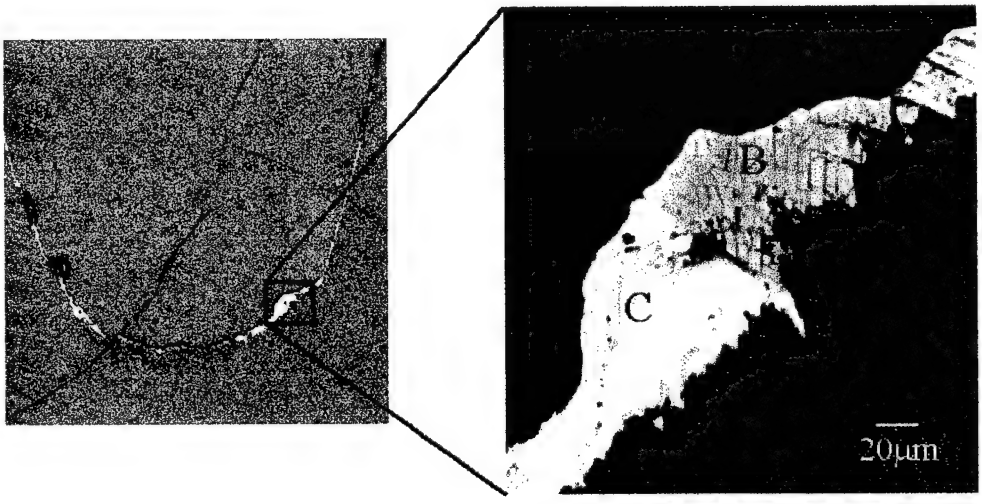

Figure 22. Inclusions formed along a grain boundary

The images in Figure 22 are from a grain boundary in boule 26 (35PT charge with 35PT seed). As can be seen from the low magnification backscatter electron image, a phase of higher average atomic number (bright phase) than the PMNT matrix (orange color) can be found along

the grain boundary. Upon further magnification, two distinct phases can be seen in the space between the grain boundary. X-ray mapping of the area performed with a JEOL JXA-733A superprobe shows that the Pb concentration remains fairly constant across the matrix phase. But, in the grain boundary the two inclusion phases show little Nb. Phase C contains Ti, and phase B contains Mg and P. The P is an impurity that should not be present in the sample, but must have been present in one of the components used to make the charge.

The superprobe was also used to perform a quantitative measurement of the phase compositions. A PMN crystal was used for a standard for Pb, Mg, and Nb concentrations, and titanium oxide was used to calibrate and standardize the Ti concentrations. Oxygen was assumed to be stoichiometric for calculation purposes, and the quantitative analysis incorporated CITZAF matrix correction algorithms. The PMNT matrix (phase A) shows the composition to be PMN-31PT . Phase B was measured to have a composition of $Pb_{1.9}Mg_{0.13}O_3$ (mostly Pb_2O_3 with a little Mg) and phase C was measured to have a composition of $Pb_{2.5}Nb_{0.018}Ti_{0.22}O_3$ (mostly PbO with small amounts of Ti and Nb). The actual data is shown in Table 2. The excess PbO in these inclusions should be similar to the flux inclusions obtained in crystals grown from PbO-based fluxes. The presence of these lead oxide phases demonstrates that a pseudo-binary phase diagram for the PMNT system does not tell the whole story of what is happening upon crystallization.

Table 2. Composition of Grain Boundary Phases based on $Pb_nTi_xMg_yNb_zO_3$

Element	Compostion of Phase A	Composition of Phase B	Composition of Phase C
Pb (n)	1.01 +/- 0.01	1.923 +/- 0.005	2.51 +/- 0.05
Ti (x)	0.309 +/- 0.004	-	0.22 +/- 0.02
Nb (z)	0.455 +/- 0.002	-	0.018 +/- 0.003
Mg (y)	0.231 +/- 0.002	0.130 +/- 0.004	-

4. Study of Structural Features in PMNT Single Crystals Using Light Scattering Tomography

Laserlight scattering tomography (LST) is a relatively new technique for looking at defects in crystals. In principle it is a simple technique. A focused, low power laser beam is directed into the crystal and light scattered from defects can observed at 90° with a microscope.

The image is recorded either on film or, as has become more common, as a video image. The scattering centers occur due to fluctuations of the dielectric constants at the lattice defects (13). Several types of defects can be identified: point defects, platelets, line defects and planar defects (13-16). The point defects are typically much smaller than the wavelength of the analyzing light and can be treated as classical Raleigh scatterers (14). The analysis of line defects is more complicated (13, 14, 16), and can be hampered by the lack of physical data for the crystal under study, in particular the dielectric constant (17). However, as the work of Sato et al (17) on proteins has demonstrated, this does not materially compromise the use of LST to study defects in crystals. The basic types of defects can be classified either by their interaction with the polarization of the analyzing light or by the angular dependence of the scattered intensity.

The in-plane resolution of LST is about 40nm (13). The out of plane (thickness) resolution is limited by the diameter of the light beam for LST (20μ). Since LST is a scanning technique, the full depth of the crystal can be probed which allows the study of defects related to the growth history of the crystal

The design of the LST apparatus involved the development of two major systems: 1) the hardware system which performs the light gathering and image storage functions, and 2) the control program which integrates the electronic functions of the apparatus and manipulates the images. The basic hardware system of the LST apparatus is shown schematically in Figure 23. This system can be further broken down into five sub-systems: the illumination system, the crystal positioning system, the imaging system, the image processing system and the computer.

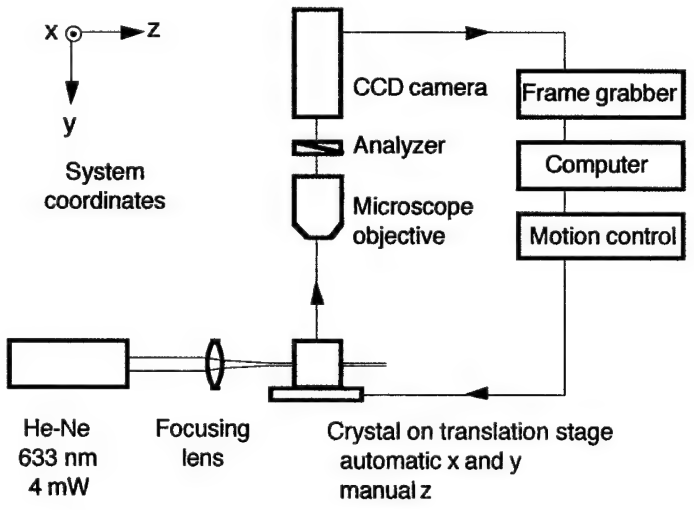

Figure 23. Schematic diagram of Laser Scattering Tomography (LST) apparatus

In operation, the crystal is scanned in the X direction and a composite image of the defects of an X-Z slice through the crystal is generated and stored in the computer. The crystal is then stepped a predetermined distance in the Y direction and the scan is repeated. Thus the entire volume of the crystal can be imaged. Using Fortner Research T3D, a 3-dimensional reconstruction of the crystal can be obtained. This reconstruction can be viewed in different ways to trace the defects through the volume of the crystal.

The LST apparatus has been used to study a number of crystals in our laboratory including strontium barium niobate (SBN), gallium arsenide (GaAs), yttrium iron garnet (YIG) fibers, and protein crystals.

When we began to section the boules of PMNT grown in our lab, it was obvious from optical microscopy that there were internal structures within the crystals. LST seemed to be the best tool to study the nature of these structures and how they propagated through the crystals. Figure 24 is a composite showing the types of information we were able to gather on these structures in PMNT. Figure 24a is a photograph of a 2mm thick slice of a PMN- 35 % PT. There is an obvious grain boundary running almost parallel to the edge of the slice. There are also hints of internal structures in the region below the grain boundary. LST scans were taken in the volume indicated by the box in figure 24a. Figure 24b shows a slice through the crystal at a depth of 600 microns below the top surface. The slice is oriented to the crystal and the first orange stripe from the top of the image is the grain boundary. There does not appear to be much organized structure above the grain boundary although there is scattering from what may be small inclusions.

Below the grain boundary, there is an organized structure. There are lines of high scattering intensity running parallel to the grain boundary (growth direction) separated by band of lower intensity. These bands are intersected by a similar set of bands running at an angle to the growth direction. These band systems are either twins and/or ferroelectric domains. There is also evidence of inclusions in this region. These small features cannot be seen with normal microscopy. Figure 24c is from a 3d reconstruction of the volume of the crystal that was scanned. It is a slice (indicated by the dotted line in figure 24a) viewed down the growth direction. The vertical dimension is exaggerated and corresponds to a 2mm height. The right of the figure corresponds to the upper surface of the slice. The region above the grain boundary shows very low scattering with some indication of the presence of inclusions. The region below the grain boundary shows the bands due to twins and/or domain penetrating into the slice. These bands are wide as they run at an angle to the plane normal. There are also isolated scattering centers, which maybe inclusions. Figure 24d shows a full 3 dimensional representation with the lower scattering intensities removed. It gives some indication of the overall distribution and shape of the structure and defects in the crystal.

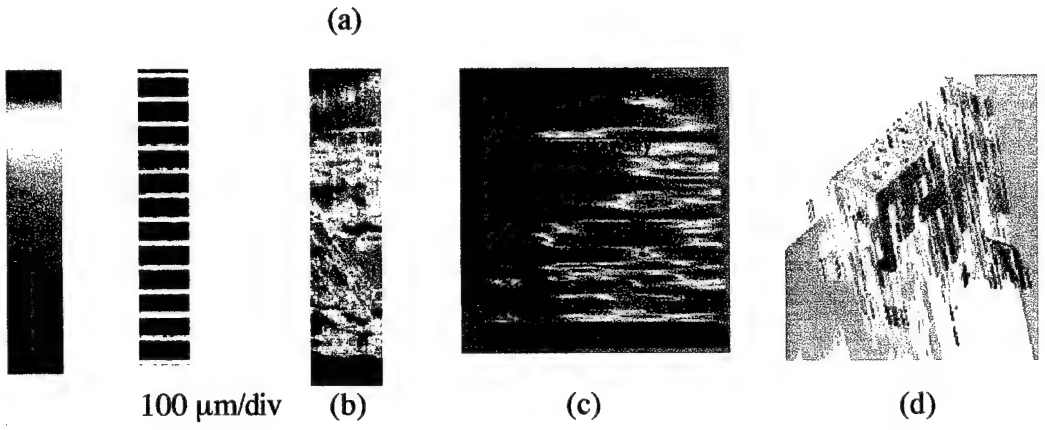

Figure 25. a) Photograph of a 2mm slice of PMN-35%PT. b) Tomograph of a section looking down from the top and at a plane below the surface (indicated by the rectangle outlined in the photo). c) Vertical cross section through the thickness (as indicated by line within the box) and taken from the 3d composite. d) 3d rendering of scattering intensity with low intensity scattering removed. The color scale on the left indicates scattering intensity (magenta being the lowest and red the highest).

One important feature of LST is that it can be used to do dynamic volumetric studies; for example, real time changes taking place during poling under different electric fields and at different temperatures. The analysis could include views in any crystallographic direction desired. This work has yet to be done. A similar study with SBN allowed us to follow the poling mechanism while varying both the poling time and the poling field. Similar studies could be undertaken for PMNT.

5. Segregation Problem in PMNT Growth

The compositional variations found along the growth axis of large diameter PMNT boules is clearly a problem. It makes it difficult to fabricate device material with uniform and optimum properties. Various samples have sent to device groups and commercial organizations with the only compositional data provided the melt composition. These might be up to 15% off the actual values. Since most of the important properties change rapidly with composition close to the MPB, it is important to find ways to grow crystals with uniform composition. The Bridgman method has an intrinsic problem with axial uniformity when melts are impure, off-stoichiometry and/or incongruently melting (such as PMNT solid solutions). The reason has to do with the presence of uncontrolled buoyancy-driven melt convection. Only under conditions of diffusion controlled growth or diffusion-like behavior can uniform composition be achieved, and this is rare in most crystal growth systems.

In normal Bridgman growth the axial temperature gradients do not encourage fluid flow (because it is colder at the interface than the melt surface). However, radial temperature gradients exist and are thought to be the dominant factor. In the smaller Pt crucibles, the convection appears to be minimal and the crystals have a fairly uniform central region. This may be due to lower radial gradients in the smaller radii crucibles, restricted flow due to more effect from wall friction or flow cells which are locally confined (uncoupled and therefore not encouraging axial mass transport). In larger crucibles, the radial gradients are undoubtedly larger since heating is from the crucible wall inward, and has further to go to reach the center of the melt. This may change the cellular flow structure and lead to more convection and mixing in the melt, accounting for the classic solute distribution found in some PMNT boules.

Using forced convection to improve crystal quality is widespread in the crystal growth industry, mostly to induce convection in a controlled manner. There are several approaches to eliminating or minimizing fluid flow in Bridgman melt configurations. One is the introduction of baffles into the melt near the interface (18,19). This is awkward, however, to accomplish in sealed Pt crucibles and at very high growth temperatures. Another approach would be to introduce a controlled "counter flow" to dampen the convective mass transport flows arising from buoyancy-driven convection.

In Bridgman crystal growth only two melt stirring techniques have been studied, accelerated crucible rotation (20-22) and low frequency vibrational stirring (23-25). In this laboratory we have been studying the latter technique and started to do some experiments toward the end of this program to see if we could improve the crystal uniformity. The method, known as coupled low frequency vibrations, and involves the application of vibrations to the crucible in such a way as to create a surface wave. The wave height and therefore the magnitude and depth of the flows are determined by the frequency used. Moving the crucible axis in a circular orbit with a variable speed motor creates the effect.

For this experiment we used a doubled walled, flat bottom Pt crucible 1.8 cm ID in diameter. It was contained in a rigid ceramic support tube within the normal growth furnace. The supports are needed to keep the crucible from tilting off axis and thereby self-destructing. The growth conditions were kept the same as before and a [111] oriented seed used. Several thermocouples were attached to the sides of the crucible for gradient and temperature measurements at the start and during growth. One of the important issue that had to be considered is the strong dependence of flow velocity and depth on melt height. As the crystal grows the melt height decreases and therefore the flow become stronger. Since our goal was only to dampen flows, not induce vigorous melt mixing, we needed to decrease the frequency continuously during growth. Since we did not have the capability at that time to do this electronically, we had to do this manually in small increments during the growth run.

The experiment, while carefully set-up, was only partially successful. First, the Pt crucible leaked somewhere near the beginning of the run and about 2 cm of melt height was lost. This meant that our calculation of the amount of stirring induced in the melt no longer applied. The result was more vigorous mixing than intended. Nevertheless, a rather large boule still resulted. The boule showed a number of interesting features not previously seen in PMNT material. These can be seen in Figure 26. The most dominant feature were striations and inclusions, neither of which have been seen in crystals of some other materials grown by this technique previously (24,25). The striations can be correlated to the small manual changes in frequency made during the growth run. While we knew that changing frequency also alters the thermal gradients in the melt and, therefore interface position, we did not know, for the PMNT system, just how far or fast the interface would actually move. For the case where the frequency

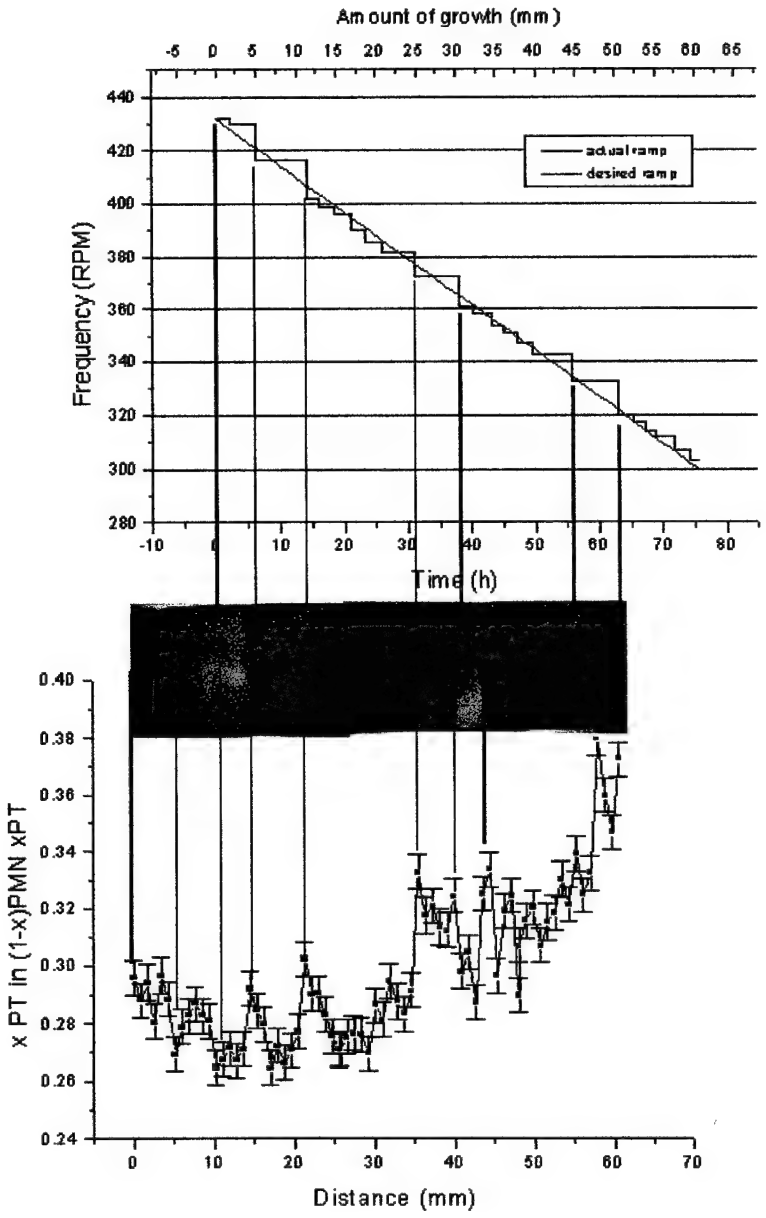

Figure 26. Results from the vibrational stirring experiment including 1) the manual changes in frequency with time, 2) a photograph showing various structural features in a thin slice along the growth axis and 3) the corresponding Ti concentration.

is lowered, the interface moves forward (enhancing growth rate). Therefore every time we made too large a downward adjustment in frequency, the growth rate jumped causing a striation.

The correlation between these frequency changes and the striations can be seen in Figure 26. Other interesting features seen in the crystal photograph include the shape of the growth interface as revealed by the striations. While they start out as symmetrical and slightly convex, about half way through the growth run they become wave-shaped, perhaps due to the flows now reaching the interface (the result of too vigorous stirring). Also found were a large density of inclusions in several regions of the boule indicating that growth rates were unstable.

Also shown in Figure 26 is the axial Ti composition profile. First, it increases continuously as in non stirred melts. Therefore this experiment did not achieve its goal of making the PMNT boule more uniform. Second there are much larger compositional variations (a peaking of the Ti concentration) over short distances along the growth axis. This is consistent with the low Ti segregation coefficient. During steady state growth, the Ti concentration normally builds up at the interface to some maximum value dependent on the details of the phase diagram. When the interface moves abruptly forward at a rapid rate it is trapped into the growing crystal. This would cause the melt ahead of the interface to be depleted in Ti and so the composition of the next grown crystal region would also be lower.

Future experiments need to be done with better control of the leaking problem and either no change in frequency during the growth run or the use of an automatic ramping program.

6. Analysis of Commercial PMNT Samples

Dr. Michael Zipparo at Tetrad asked us to look at two commercial single crystal samples they received one of which had good physical properties (labeled here as No.1), and the other poor (labeled No.2) . They were both bar-shaped as shown in Figure 27a. The good sample had a uniform appearance under crossed polarized light while the other showed a lot of structure as seen in Figure 27a, including a possible grain boundary and various types of inclusions (black and various shades of orange). The stripes may be either domains or twins. This sample may have been depoled at some point in its fabrication or testing. In addition there was some difference in the Ti concentration between the two samples, as can be seen in Figures 28. The good sample had both a more uniform composition, centered at about 30-31% PT, while the poor sample had a larger point to point variation averaging up to 2% PT higher. So long as the material

remains single phase in the rhombohedral region, the properties of Sample 2 should actually improve as the Ti content increases. Therefore it seems likely that the structural features in this sample are probably responsible for the poorer properties.

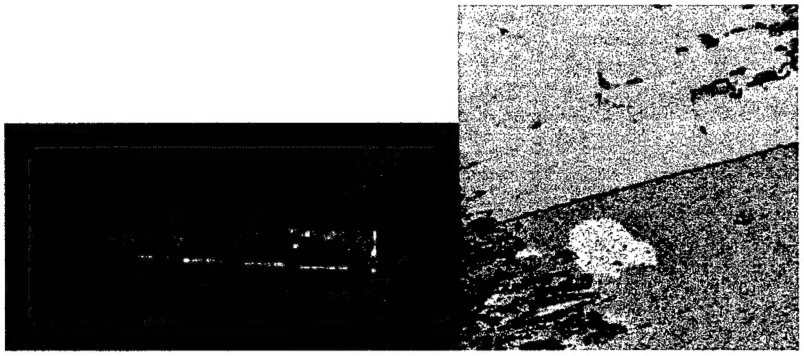

Figure 27. (a) Photograph of the commercial sample having poor properties (#2) (optical microscopy under crossed polarizers). and (b) a backscattered electron picture showing a detail of the structure in the stripped region on the right

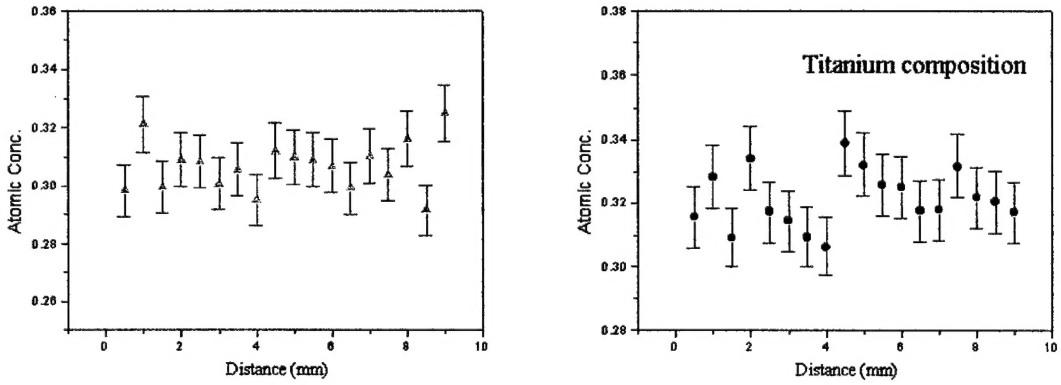

(a) (b)

Figure 28. Ti concentration along the bar length magnified a) commercial sample 1 and b) commercial sample 2.

CONCLUSIONS

We were the first to demonstrate that the Bridgman method could be used to grow single crystals of PMN and a variety of compositions in the PMN-PT system from the melt. Boules up to 1 inch diameter were successfully grown. We were the first to show that in larger PMNT crystals the Ti concentration varied with fraction solidified, in agreement with the case of unidirectional

solidification with complete melt mixing. For a 35% PT melt, the composition can range from 30% to over 40% PT in the main part of the boule . The use of oriented seed crystals facilitates the growth of single crystal boules. The fast growth direction was determined to be the [111] direction. As the Ti concentration increases, as-grown boules exhibit different light scattering behavior. Compositions around 30% PT appear cloudy from scattering off domain and/or phase boundaries. Material in the tetragonal region is clearer with larger, more visible domain/twin features.

We have found that single crystal regions with compositions near the MPB contain a two phase regions consisting of both the tetragonal and rhombohedral phases. The width of this homogeneity region seems smaller that the ceramic data reported by Kelly et al (12), and may be related to the processing conditions and how much they deviate from equilibrium conditions. The properties of single crystals seem to depend largely on composition, however our analysis of some commercial samples of nominally the same composition indicated that structural features may play an important role also. This should be explored further.

One experiment was carried out to see if we could improve compositional uniformity by suppressing buoyancy driven convection with a counter forced convection (using a vibrational stirring method). The results were inconclusive as the processing conditions were not optimized

We have collaborated with a number of other groups being supported by ONR and DARPA and either supplied them with crystal samples, advice on crystal growth or analysis of their samples. One of our foreign visiting scholars, Dr. Sang-Goo Lee, who worked with us on this program started his own company to grow these materials.

REFERENCES

1. S.-G. Lee, R.G. Monteiro, R.S. Feigelson, H.S. Lee, M. Lee, S.-E. Park. Appl. Phys. Lett. 74 (1999) 1030.
2. R.F. Service. Science 275 (1997) 1878.
3. S.-E. Park, T.R. Shrout, J. Appl. Phys. 82 (1997) 1804
4. W.A. Bonner and L.G. Van Uitert, *Mat. Res. Bull.*, 2 (1967) 131
5. F. J. Kumar, L. C. Lin, C. Chilong, M.J. Tan, J. Crystal Growth 216 (2000) 311
6. Sandrine Gentil, Gilles Robert, Nava Setter , Paul Tissot, Jean-Pierre Rivera, Jpn. J. Appl. Phys. 39 (2000) 2732

7. Tsuyoshi Kobayashi, Senji Shimanuki, Shiroh Saitoh and Yohachi Yamashita, Jpn. J. Appl. Phys. 36 (1997) 6035
8. Z-G Ye, M. Dong, Y. Yamashita, J. Crystal Growth 211 (2000) 247
9. M. Dong, Z-G Ye, J. Crystal Growth 209 (2000) 81
10. K. Harada, Y. Hosono, S. Saitoh and Y. Yamashita, Jpn. J. Appl. Phys. 39 (2000) 3117
11. S.L. Swartz, T.R. Shrout, Mater. Res. Bull. 17 (1982) 1245
12. J. Kelly, M. Leonard, C. Tantigate, A. Safari. J. Am. Ceram. Soc. 80 (1997) 957
13. K. Moriya and T. Ogawa, *J. Crystal Growth* **44,** 53 (1978)
14. K. Moriya and T. Ogawa, *Phil. Mag.* **A41,** 191 (1980)
15. K. Moriya and T. Ogawa, *Phil. Mag,* **A44,** 1085 (1981)
16. F. Thibault, J. Langowski and R. Leberman, *J. Crystal Growth* **122,** 50 (1992)
17. K.Sato, Y. Fukuba, T. Mitsuda, K. Hirai and K. Moriya, *J. Crystal Growth* **122** 87 (1992)
18. C. Marin, A.G. Ostrogorsky. J. Crystal Growth 211 (2000) 378
19. P.S. Dutta, A.G. Ostrogorsky. J. Crystal Growth 191 (1998) 904
20. H.J. Scheel. J. Crystal Growth 13/14 (1972) 560
21. H.J. Scheel, E.O. Schuz-Dubois. J. Crystal Growth 8 (1971) 304
22. A. yeckel, J.J. Derby. J. Crystal Growth 209 (2000) 734
23. W.-S. Liu, M.F. Wolf, D. Elwell, R.S. Feigelson. J. Crystal Growth 82 (1987) 589
24. Y.-C. Lu, J.-J. Shiau, R.S. Feigelson. J. Crystal Growth 102 (1990) 807
25. R.C. DeMattei, R.S. Feigelson J. Crystal Growth 128 (1993) 1062

VII. APENDICES

A. Publications and Presentations

1. "Growth and Characterization of High Quality Lead Magnesium Niobate Titanate Single Crystals", M.C.C. Custodio, Y.T. Fei, K. Zawilski, R. DeMattei and R.S. Feigelson, Presented at the12th IEEE International Symposium on the Applications of Ferroelectrics - ISAF 2000, Honolulu, Hawaii, August, 2000.

2. "Growth of Lead Magnesium Niobate Titanate Single Crystals For Electrooptic and Piezoelectric Applications", M.C.C. Custodio, Y.T. Fei, K. Zawilski, R. DeMattei and R.S. Feigelson, Presented at the 2nd International Symposium on Laser, Scintillator and Nonlinear Optical Materials, Lyon, France, May, 2000.

3. "Growth and Characterization of High Quality Lead Magnesium Niobate Titanate Single Crystals", M.C.C. Custodio, Y.T. Fei, K. Zawilski, R. DeMattei and R.S. Feigelson, Presented at the 2000 US Navy Workshop on Acoustic Transducers, State College, Pennsylvania, April, 2000.

4. "Growth and Characterization of PMN and PMNT by the Bridgman Method", S. G. Lee, R. G. Monteiro, M. C. C. Custodio and R. S. Feigelson, Presented at the 11th American Conference on Crystal Growth and Epitaxy, in Tucson, Arizona, August, 1999.

5. "Growth and Characterization of Pb(Mg1/3Nb2/3)O3 and solid solution with $PbTiO_3$ by the Bridgman Method", S. G. Lee, R. G. Monteiro, M. C. C. Custodio and R. S. Feigelson, Presented at the 1999 US Navy Workshop on Acoustic Transducers, State College, Pennsylvania, April, 1999.

6. "Growth and electrostrictive properties of $Pb(Mg_{1/3}Nb_{2/3})O_3$ crystals", Sang-Goo Lee, Ralph G. Monteiro, Robert S. Feigelson, Howard S. Lee, Myeongkyu Lee, Seung-Eek Park, Appl. Phys. Lett., vol. 74, no7 (1999) 1030-1032.

B. Program Participants

Staff:

Dr. Robert C. De Mattei

Visiting Scholars:

Dr. M. Claudia Custodio

Dr. Yi-Ting Fei

Dr. Sang-goo Lee

Students:

Howard Lee Ph.D. awarded 1999

Myeongkyu Lee Ph.D. awarded 1998

Ralph Monteiro M.S. awarded 1999

Kevin Zawilski Ph.D. anticipated 2003